Marine Structures 99 (2025) 103698

Contents lists available at ScienceDirect

Marine Structures

journal homepage: www.elsevier.com/locate/marstruc

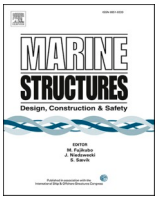

Numerical assessment of marine hose load response during reeling and free-hanging operations under Ocean waves

Chiemela Victor Amaechi [a,b,c,*], Ahmed Reda [d,e,**], Mohamed A. Shahin [d], Charles Agbomerie Odijie [f,***], Salmia Binti Beddu [c], Daud bin Mohamad [c], Agusril Syamsir [c], Idris Ahmed Ja'e [c,g], Xuanze Ju [h]

[a] School of Engineering, Lancaster University, Lancaster, Lancashire, LA1 4YR, UK
[b] Department of Construction Management, Global Banking School, Devonshire Street North, Manchester, M12 6JH, UK
[c] Institute of Energy Infrastructure, Universiti Tenaga Nasional, Jalan IKRAM-UNITEN, 43000, Kajang, Selangor, Malaysia
[d] School of Civil and Mechanical Engineering, Curtin University, Bentley, WA, 6102, Australia
[e] Cladtek International PTY LTD, Perth, Australia
[f] Engineering Department, MSCM Ltd., Coronation Rd, High Wycombe, Oxfordshire, HP12 3TA, UK
[g] Department of Civil Engineering, Ahmadu Bello University, Zaria, 810107, Nigeria
[h] Offshore Oil Engineering Co., Ltd., Engineering Company, Tianjin, 300451, China

ARTICLE INFO

Keywords:
Marine hose
Finite element modelling
Marine risers
Reeling hose
Offshore platforms
Marine structures
Ocean waves

ABSTRACT

In recent times, the need for sustainable fluid transfer has necessitated the application of bonded hoses and composite risers. It has been considered increasingly within the marine-offshore industry, with advances in loading/offloading operations, and newer offshore platforms. This paper presents a reeling study under different operational and environmental conditions. In this study, finite element modelling (FEM) was used for the design of marine bonded reeling hoses, and two wave spectra were applied to two reeling hose operations. The design assessed the load response of the marine bonded hoses during two different operations, including free-hanging (static) and reeling (dynamic/loading), and assessments were made for reinforced and mainline hoses. The findings aid an understanding on the load response, tension profiles, stress profiles, strain distribution and hose curvature of marine reeling hoses. The study showed different fluid contents affect the performance of the hose differently parametrically. It justifies the use of design specifications for reeling hose under the operation modes for marine application. The recommendations obtained from this study can assist in developing standards and guidance for use by marine hose designers and manufacturers.

Abbreviations:

2D – Two Dimensional
3D – Three Dimensional
6D – Six Dimensional
GoM – Gulf of Mexico
HEV - Hose End Valves
H_s - Significant wave height

(*continued on next page*)

* Corresponding author. School of Engineering, Lancaster University, Lancaster, Lancashire, LA1 4YR, UK.
** Corresponding author. School of Civil and Mechanical Engineering, Curtin University, Bentley, WA, 6102, Australia
*** Corresponding author.
E-mail addresses: chiemelavic@gmail.com (C.V. Amaechi), ahmed.reda@curtin.edu.au (A. Reda), charlesodijie@hotmail.com (C.A. Odijie).

https://doi.org/10.1016/j.marstruc.2024.103698
Received 11 November 2021; Received in revised form 11 April 2024; Accepted 25 September 2024
Available online 2 October 2024

(*continued*)

6DoF - Six degrees of freedom	HSE – Health & Safety Executive
A - Area of the body	ID - Inner Diameter
ABS – American Bureau of Shipping	ISO - International Organization for Standardization
API – American Petroleum Institute	JONSWAP - Joint North Sea Wave Project
APS - Accumulated Plastic Strain	MBC - Marine Breakaway Couplings
BM – Bending Moment	MCI - Metal-Composite Interface
CALM - Catenary Anchor Leg Mooring	MBR - Minimum Bend Radii
CPU – Central Processing Unit	MLP - Mechanically-Lined Pipes
Curv. - Curvature	MWL - Mean Water Level
DAF – Dynamic Amplification Factor	OCIMF - Oil Companies International Marine Forum
DAF_{hose} - Dynamic Amplification Factor of Hose	OD - Outer Diameters
DNVGL - Det Norkse Veritas & Germanischer Lloyd	OLL – Offloading Lines
DP- Dynamic Position	PSA - Petroleum Safety Authorities
ET – Effective Tension	RAO - Response Amplitude Operators
FEM- Finite Element Modelling	STS - ship-to-ship
FPSO – Floating, Production, Storage and Offloading	t – time or simulation time steps
GMPHOM – Guide to Manufacturing and Purchasing Hoses for Offshore Moorings	T_p – Peak period
	UK – United Kingdom

1. Introduction

With the increasing demand for oil exploration in deep waters, there are advances needed in composite materials. Recent times have seen marine hoses, composite risers, and composite pipes as increasingly common applications in the offshore industry due to their considerable popularity ([1–4]). This is due to the properties of composites that can be harnessed, such as strong flexibility and corrosion resistance, making them easier to use, transport, install, maintain, and operate [2,4,5]. Additionally, composites are lightweight materials that help to lessen the deck weight of offshore platforms. Other important aspects include the stability and motion of the Floating Production, Storage, and Offloading (FPSO) vessels, which also affects the performance of the marine hose system when the floating platform is moored [6–8]. Earlier study by Amaechi et al. [9] considered the strength performance of submarine hoses that were connected to the Catenary Anchor Leg Mooring (CALM) buoy using numerical modeling approach of coupling the hydrodynamic loads and proposed the use of the DAF_{hose}. Although, other recent studies have shown that offshore structures like umbilical cables, flexible risers, composite risers and marine hoses are multi-layered [1–4,9], they are influenced by various parameters such as winding angles, number of cord layers, helix steel wire pitch, inner diameter, and layer thickness underneath the helix steel wire [9–13]. Therefore, there is a need to consider the loading operation during the design of the marine hoses following various findings [14–18].

Recent reel-lay pipeline installations have been reported as a highly cost-effective method being applied in the industry ([19–21]). Thus, another justification for the utilization of marine bonded hoses as an adaptable techno-economic marine approach is its flexible composition of marine hose lines and the increasing demand for more sustainable structural conduits to transport fluids [1,22–25]. However, sometimes, these hoses crash when reeled due to the connections and valves. In principle, the application of reeling requires a reeling drum and a hose material that goes around it [26–28]. The reeling technology is to conserve space for marine operations

(a) vertically positioned (b) horizontally positioned

Fig. 1. Typical configuration of FPSO-mounted reeling system, the reeling vessel, reeling hoses, and reel drum, showing (a) the reeling hose end being vertically positioned and (b) the reeling hose end being horizontally positioned.

while still being able to have adequate length of the flexible hose material for different marine operations. This could be a ship-to-ship (STS) catenary connection, hose discharge connection, reeling hose spooling, or free-hanging. However, reeling hoses can be positioned along different directions from the reel drum due to their flexibility, as depicted in Fig. 1.

In reality, the reeling technology has been applied in domestic garden hoses, fire hoses, road excavator hoses, pipe bending, spooling of hoses, pipe laying using a reel-lay system, and marine reeling hoses. The marine reeling hoses are usually bonded hoses with comparatively longer section lengths but larger inner bore diameters and thicker hose walls. Despite the short service life of these hose types, they offer cost-saving advantages over other conventional technologies. They also save space via reeling and are rate-saving in terms of the time for laying the hose line (or pipeline) on the seabed. However, these marine hoses have been reported to have some issues such as early damage in some captured failure modes ([27,29]). Structurally, the reeling operations involve a combination of forces like torsion and tension [27,30,31] and the reeling modelling is usually conducted based on the well-validated reeling mechanics proposed by Focke [30]. Manouchehri [31] presented a reeling pipeline model for lined pipes with its deployment and application on the pipelaying vessel. However, these reeling studies were limited to general offshore pipelines and did not include any reeling hoses. Chesterton [27] presented the local design and global design of the reeling hoses but looked at a single case of the hose, alongside that it did not consider the hose behaviour at interfacial layers, or structural verification at each particular hose section. In his global design of the hose model, the JONSWAP wave spectrum was usually applied but the free-standing and reeling operations were not considered for different wave conditions. However, some hose behaviour was observed from the helical spring-like reinforcements on the liners, called liner wrinkling. Another instance of hose failure from the helix was reported by Lassen et al. [32]. In this case, it was found that the hoses have issues with high strains observed in the hose structure. It was stated explicitly to have a standard for reporting both layer delamination and reinforcement helix rupture, thus some helix fatigue tests can be conducted on helix sections, as reflected in their suggestion. The study by Lassen et al. [32] opened up the conversation that there has been some concern based on the reliability of these marine hoses under extreme load conditions, during long-term use in service and during reeling. This means that marine reeling hoses are susceptible to damage due to operation (usage), storage and also self-weight when reeling. Another issue reported is that there are also some crush load effects on the hose from the end-fittings, couplings and valve connections, such as the Hose End Valves (HEV) and Marine Breakaway Couplings (MBC).

In a recent study, Ju et al. [33] developed a numerical model of a CALM buoys with moored tanker system, and found the effect of pullback force hawser capacity, buoy kissing, and fishtailing motion, and recommended the need to have a tug present always whenever a tanker is moored to the CALM system, however that study did not consider any hose or mooring failure. In some CALM buoy cases, the failure of one mooring chain within the single point mooring (SPM) could result in hose failure [34–38]. One key justification for this study is presenting other methods of assessing the strength of the reeling hoses and improving the findings on these marine structures, for better utilization in the field by end users. The Petroleum Safety Authorities (PSA) in Norway earlier made some investigations into the design, reliability and in-service experience for different flexible risers and marine hoses (see PSA reports [22,25]). These reports presented some failures on unbonded flexible risers and bonded flexible risers (marine hoses). Due to this fact, it is often required to design the marine hoses according to industry standards like API 17K [39], which is the Specification for Bonded Flexible Pipes. The API 17K standard document requires an accurate determination of the load response in the hose wall which is not the case with the industry's main specification–Oil Companies International Marine Forum (OCIMF)'s GMPHOM [40] guidelines. The stress and strain response in the hose have to be determined layer-by-layer in the hose wall's composite structure, for both extreme load response and fatigue life prediction purposes. This approach combined with relatively low permissible utilization ratios would ensure design safety and reliability. This approach also requires an in-depth analysis, industry expertise alongside specialist design experience on marine hoses. In other words, there are currently no available literature that comprehensively looked into the load response and utilization ratios of these marine hoses. Nevertheless, different operation conditions of marine hoses have also been reported over the past decades, such as the loading and offloading operations ([41–45]). Due to the importance of offshore structures, a range of works have looked into their strength performance, stability, standards, cost efficiency, motion, offloading operations as well as response behaviour [46–54]. Whilst the study by Santos, and Guedes Soares [41] investigated on optimizing the cost for offloading operations via shuttle tankers, another study by Chen et al. [55] investigated direct offloading operations using dynamic positioned (DP) shuttle tanker, however both studies did not consider reeling operations. In that light, these various operations require efficient systems and well validated offshore materials like offshore composites [1,5,23]. Considering the range of industry standards for these offshore structures [39,50,52,54,56], there is a rise in material development and improved techniques in the industry [34,49,57–59].

From the literature search, there are no studies that compare the strengths of reeling hoses to the strengths of either floating hoses or submarine hoses. However, some recent marine hose studies were used to assess the strength of submarine hoses [9,11]. These were carried out by considering the hydrodynamic loads on the hose models attached to a Catenary Anchored Leg Mooring (CALM) buoy in Lazy-S and Chinese-lantern configurations. It was moored by six catenary mooring lines and the study proposed some guidance factors on the dynamic amplification factors of hoses (DAF_{hose}). However, the study did not consider the operational conditions for reeling or spooling and did not also have reeling configurations, thus the need for the current investigation. Moreover, the impact of ocean waves and wave-induced stresses on offshore structures have been investigated by various researchers to develop better materials, and improve the overall performance of offshore structures [60–64]. Particularly, there are different models which have also been presented on the dynamic analysis of offshore reel-laying and pipe-laying operations [14,30,57,58]. Zhao and Hu [17] numerically investigated the detachment and wrinkling behaviour of mechanically-lined pipes (MLPs) considering the spooling-on stage to the reel indicating that MLPs critical spooling-on curvature increased by over 47 %. They also found that the curvature reached 0.1432 rad/m when the wall thickness of the outer layer increased from 14.3 mm to 17.9 mm. In an earlier study by Castello and Estefen [61], the limit strength and reeling effects of sandwich pipes with bonded layers were presented using two sandwich pipes composed of steel layers and separated by a polypropylene annular. The investigation was aimed at the effect of interlayer adhesion and the ultimate

strength under external pressure and longitudinal bending. It was concluded that the ultimate strength of the sandwich pipe is strongly dependent on the shear stress acting at the interface. These studies showed different parameters that could be investigated on marine hoses and reeling pipes. However, such studies did not consider the effect of the vessel, strain estimation parameters, wave heading on environmental factors, and reeling behaviour under fluid loads, thus the need for the current investigation.

In the current study, finite element modelling is used for the assessment of marine hoses under two operations, namely free-standing (static) and reeling (dynamic). The study aims to understand the load response, tension profiles, stress profiles, strain distribution, and hose curvature of marine reeling hoses. In addition, this study presents parametric relationships that influence the load response of the bonded hoses and aid in the safe operation of envelopes.

2. Global design of current model

2.1. Description

For the global design of the current model, the full case of the reeling operation was considered and modelled using the software Orcaflex [65]. This software is specialised in modelling and simulating subsea and floating systems in different ocean conditions. Vessel motion was considered a factor that can induce some dynamics on the reeling hose. The purpose of the global analysis was to simulate the reeling process as a whole system rather than just focusing on certain sections of the riser pipeline. The simulation was used to obtain the mechanical data in real-time as the pipeline was reeled in. Data including the effective tension, stress, bending moment, and curvature were recorded. The model was set up using Floating, Production, Storage, and Offloading (FPSO) of a similar reeling vessel with reels. The model was carried out to ascertain the different physics investigated on the loading conditions of the marine reeling hose and to present results from both static and dynamic behaviour of the reeling hose. The global finite element consists of a transfer hose connected between the reeling FPSO or reeling floater and subsea buoy location, as illustrated in Fig. 2. The parameters of the reeling hose model are presented in Table 1.

2.2. Reeling operation

The finite element modelling (FEM) software called Orcaflex was used to simulate the reeling operation. A long section of the bonded hose was developed for different operations, as illustrated above in Fig. 2. The reeling hose was reeling on the reeling drum and a roller was used to control the path. The reeling operation (also called the spooling operation) was considered as it involves tensioning and the hose was bent onto the reel drum plastically, which creates the highest curvature during the reeling process [30,31,66]. The reeling hose can be used for pipe-laying operations too from the position above mean water level (MWL) down to the seabed. However, in this case, the reeling operation does not include laying.

2.3. The free-standing operation

The free-standing operation was also considered using the FEM software called Orcaflex. Also, a section of the lengthy reeling bonded hose was developed, as illustrated above in Fig. 2 (b). The reeling hose was left free to hang-off the reel drum of the vessel. Due to the weight of the HEV and tail-end hose section, the free-hanging hose-string is subject to the hose which acts under gravity as it is

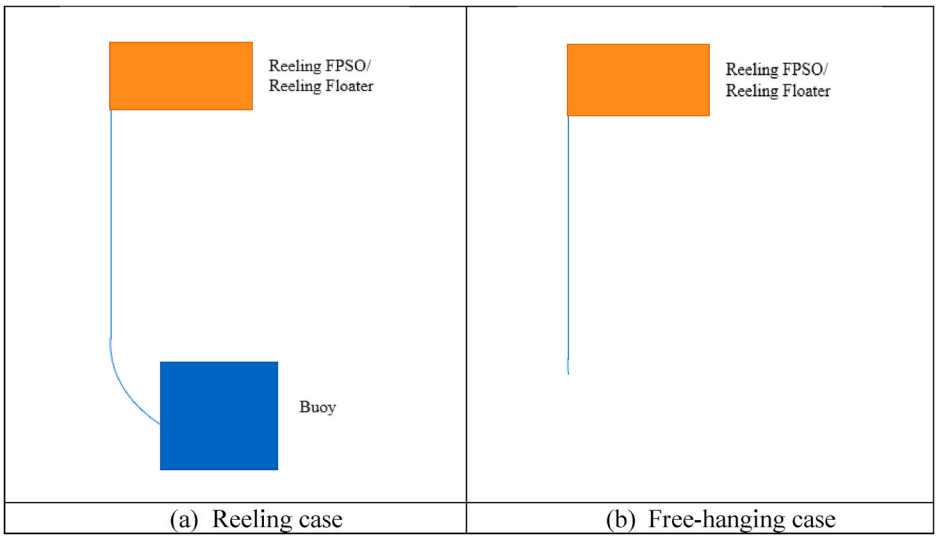

Fig. 2. Simplified schematic of the model showing: (a) reeling; and (b) free-handing cases.

Table 1
Parameters for the reeling hose model used in the current study.

Parameter	Value (m)
Hose outer radius	0.52
Hose inner radius	0.49
Length of hose section	12.0
Length of hose-string	350.0
Radius of reel	3.00
Outer reel radius	0.11
Tensioner radius	0.02

straight in 180°. While the free-hanging operation requires some hose sections but it also it also involves tensioning and bending, which creates some curvature but minimal curvature during the process, as that end is not restrained but free on that end. Due to the swivels on the HEVs at the end of the marine hose, it is pertinent to have some understanding on the mechanics of free-standing risers, which are available in literature [26,46].

2.4. Wave loads and ocean conditions

In the current model, the wave motion was set such that there was negligible wave height and that any wave motion was acting directly towards the bow of the ship, not at an angle to the ship. The inputs for the current and wind speeds were all also set to negligible amounts. Displacement Response Amplitude Operators (RAO) and harmonic motion were superimposed in the analysis. To obtain the global design, the ocean conditions were considered to suit the reeling condition in the FEM for the reeling hose. The ocean conditions used to obtain the model are shown earlier in Fig. 2 and given in Table 2.

2.5. Environmental conditions

For the environmental conditions, three different cases were considered in this study, as presented in Table 3. The numerical model was performed under the Torsethaugen and Haver wave spectrum and JONSWAP wave spectrum. These two wave spectra which were employed in this study have related characteristics. These wave spectra suit well for oceans around West Africa and the North Sea. This wave type can also carry out irregular waves and thus its wave spectrum was considered in this model, as shown in Fig. 3. Further initial conditions were set for the first case (Case1), for the environmental factors that the non-operational and the operational modes. The initial factors were set such that there was minimal wave motion, current speed or wind speed to affect the system. The design consideration used four positions of the FPSO, given in Table 4.

2.6. Wind and current loads

The coefficients of wind and current loads used for the 6DoF cylindrical FPSO, alongside corresponding parameters used are tabulated in Table 5. The uniform current profile was used to estimate the current and wind loads which were applied to the model. Air has a density of 1.225 kg/m^3 (0.001225 g/cm^3) at sea level and 15 °C. The current speed was set to 0.5 m/s, while the wind speed was set at 22 m/s. The XY axes were used to describe the current profile for the surface current and seabed current, as shown in Table 5. The surface current speed was calculated using Orcaflex 11.0f through an interpolated current profile, which had to be larger than or equal to the current speed at the seabed. The lowest frequency (fundamental frequency) used in the study was 0.06048 Hz.

3. Materials and methodology

3.1. Materials

The materials considered in the current model were selected following the specifications in OCIMF GMPHOM [40] and API 17K [39], as the hose materials must be of high strength potential and high corrosion resistance. As such, the hose line, which is similar to a

Table 2
Ocean and seabed parameters in the current study.

Parameter	Value
Water Density (kg^{-3})	1025
Ocean Kinematic Viscosity (m^{2}s^{-1})	1.35 X 10^{-6}
Wave Amplitude (m)	0.145
Seabed Stiffness (kNm^{-1}m^2)	100
Ocean Temperature (°C)	10
Water Depth (m)	400
Seabed Model Type	Elastic Linear

Table 3
Environmental wave loads for the wave spectra.

Case Number	Hs (m)	Tp (s)	Wave Angle (°)
Case1	5.5	14.0	90
Case2	5.5	14.0	180
Case3	5.5	14.0	270
Case4	5.5	14.0	360
Case5	5.5	16.0	90
Case6	5.5	16.0	180
Case7	5.5	16.0	270
Case8	5.5	16.0	360

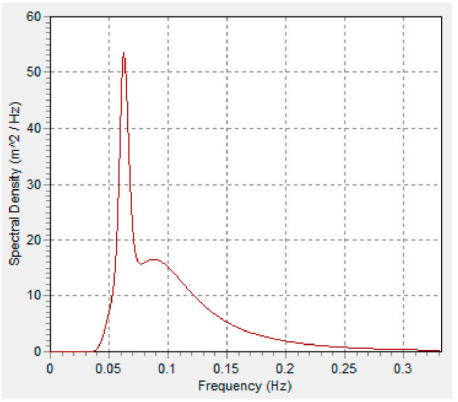

(a) Spectral density for Hs = 5.5m Tp = 16s using Torsethaugen and Haver spectrum

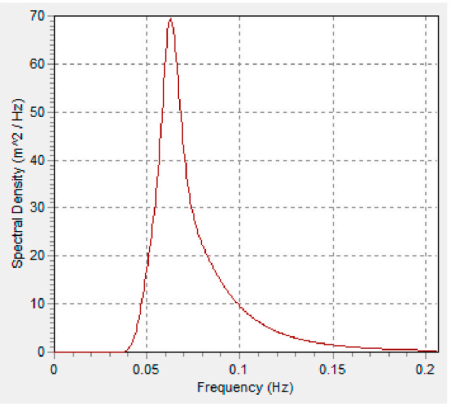

(b) Spectral density for Hs = 5.5m Tp = 16s using JONSWAP spectrum

Fig. 3. Environmental conditions showing the (a) Torsethaugen and Haver, (b) JONSWAP wave spectra.
(a) Spectral density for Hs = 5.5m Tp = 16s using Torsethaugen and Haver spectrum
(b) Spectral density for Hs = 5.5m Tp = 16s using JONSWAP spectrum.

Table 4
Position of FPSO considered.

Position	Description of Activity
P01	1st Weathervane Position
P02	2nd Weathervane Position
P03	1st Automated DP Position
P04	2nd Automated DP Position

Table 5
Wind and current parameters.

Parameters	Value	Unit
Air density	1.23×10^{-3}	kgm^{-3}
Air kinematic viscosity	15.0×10^{-6}	m^2s^{-1}
Current speed	0.0	ms^{-1}
Current direction	180	deg.°
Current method	Interpolation	–
Wind type	Constant	–
Wind speed	0.0	ms^{-1}
Wind direction	0.0	deg.°

marine riser or pipeline, must be fit for its purpose [9,47]. Thus, the material properties selected for the reeling hose have been obtained from various sources in literature [28,48,49]. Thus, it is pertinent to give the mechanical properties for the marine hose (see Table 6 and Fig. 4).

Table 6
Mechanical properties considered for the hose.

Hose Component	Material	Density (kg. m^3)	Tensile Yield Strength (MPa)	Tensile Ultimate Strength (MPa)	Elasticity Modulus (MPa)	Poisson's Ratio
Fibre reinforcement	Polyester	1200	128,000	148,000	3500	0.42
Steel Helix wire	82B Steel	7800	250,000	250,000	210,000	0.30
2nd reinforcement	Neoprene	1230	11.88	14.84	20.00	0.49
Wire/rubber laminate	Nitrile rubber	1000	15.00	20.00	15.00	0.49
1st reinforcement	Nitrile rubber	1000	24.10	25.00	18.00	0.49
Cover	Closed-cell foam	33.00	15.00	15.00	10.00	0.50

Sources: [28,48]; Matweb [49]

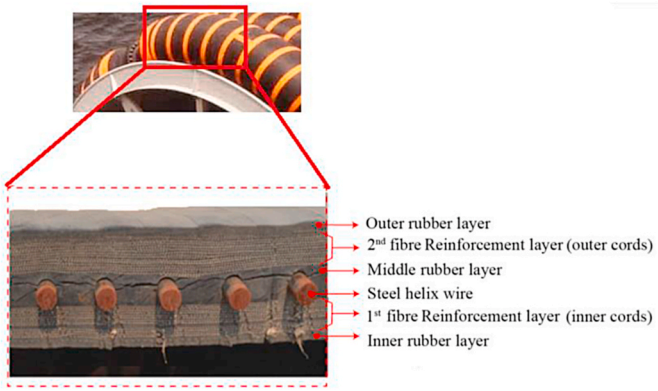

Fig. 4. Typical cross-section of marine hose showing its layers.

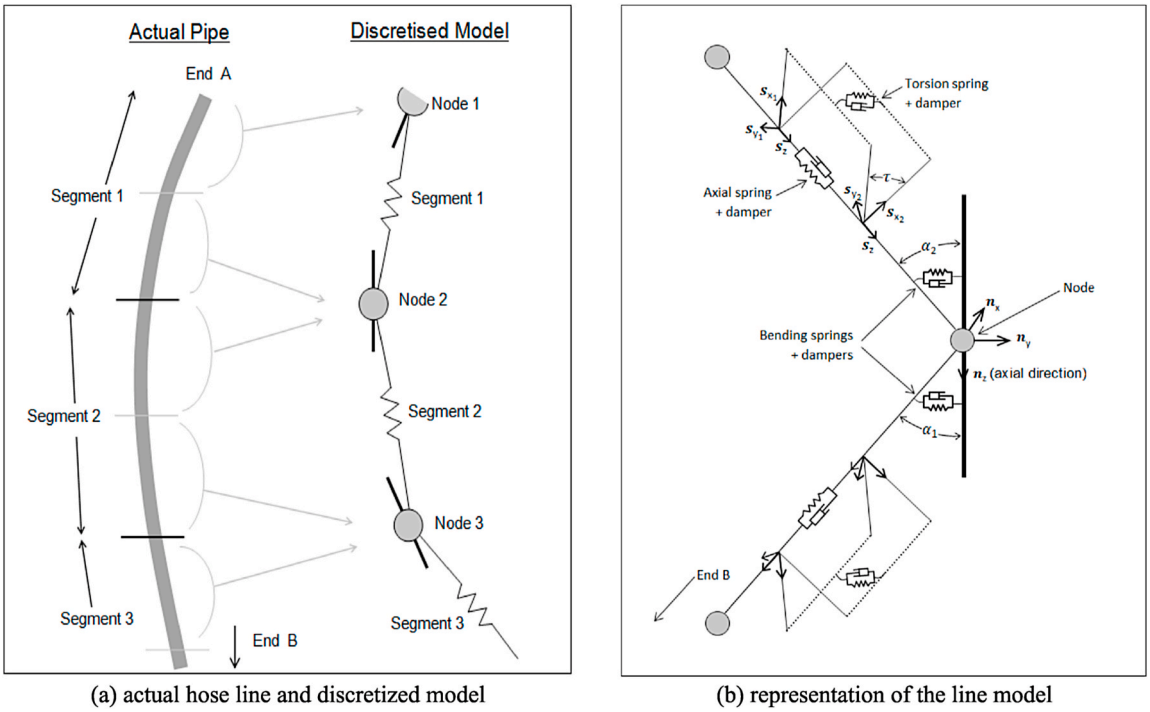

(a) actual hose line and discretized model (b) representation of the line model

Fig. 5. Orcaflex line theory showing: (a) actual hose/main line and discretized model; and (b) detailed representation of the line model (courtesy of [65,67]).

3.2. Design load conditions

The global design of the reeling hose model was considered to follow the industry design standards for bonded pipes, in API 17K [39] and OCIMF's GMPHOM [40]. For a successful reeling operation, constraints were used as the boundary. In terms of path, the constraints were developed based on the contacts and the directions of forces being applied to the system. In this present analysis, the fluid content was considered. The analysis was based on the structural integrity and strain of the reeling hose. However, during the operation of the bonded hose lines, the structure of the asset was subjected to internal pressure, external pressures and vessel motion. The static and dynamic analysis were applied in simulation, in the method of analysis using two scenarios: loading and free-hanging operations.

3.3. Orcaflex line theory

The Orcaflex line theory is depicted in Fig. 5. It shows three different spring dampers that exist in the Orcaflex line model. These are the axial, the bending and the torsional spring dampers. The axial stiffness and damping of the line are modelled by the axial spring-damper at the centre of each segment, by applying an equal and opposite effective tension force at the nodes on each end of the line segment. The bending behaviour is depicted by rotational spring-dampers at either side of the node, which spans between the node's axial direction and the segment's axial direction. The third is torsional and it is optional. If torsion is included, then the line's torsional stiffness and damping are modelled by the torsional spring-damper at the centre of each segment, which applies equal and opposite torque moments to the nodes at each end of the segment. The inclusion of the torsion implies that the torsional spring damper is unavailable in the model and the two halves of the segment are then free to twist relative to each other. The reeling hose was designed using the software Orcaflex [65].

3.4. Model components

Hose: The strength of the hoses was assessed using the API 17K standard [39,50]. The hose model considered is illustrated in Fig. 6 and described in Table 7. It shows the description of a typical marine reeling hose model designed for offloading and discharge hose. Details on the maximum utilization required for the hose capacity during normal operating conditions are presented later. Fig. 7 shows the hose markings with a description.

Floating, Production, Storage and Offloading (FPSO): Cylindrical FPSO was designed for this reeling study and the calculation included the superimposed motion of displacement RAO and harmonic motion. The cylindrical FPSO has a diameter of 56.0m, a height of 50.0m and a draft depth of 20.5m, as detailed above in Table 8. The reeling study was carried out in two operations: reeling and free-hanging. Thus, one case of the FPSO was developed in the absence of the following parameters: primary motions, wave loads, wave drifts, added mass, damping or static included in the FPSO vessel calculation. The type of FPSO was for storage and offloading purposes, as well as reeling off the hose. The cylindrical FPSO has 6DoFs (six degrees of freedom), as presented in Fig. 8, while the Orcaflex model is shown in Fig. 9.

Reel: The reel was designed as a 6D buoy using an elastic solid shaped as a curved plate, with a reel profile given in Table 8 and shown in Fig. 9, while the details of the parameters for the reel are given in Table 9 and Table 10.

Wave heading: An important aspect of this study is the application of the wave heading and the direction of the reel-mounted FPSO vessel. For illustrative purposes, the wave directions on the cylindrical-shaped FPSO are depicted in Fig. 10.

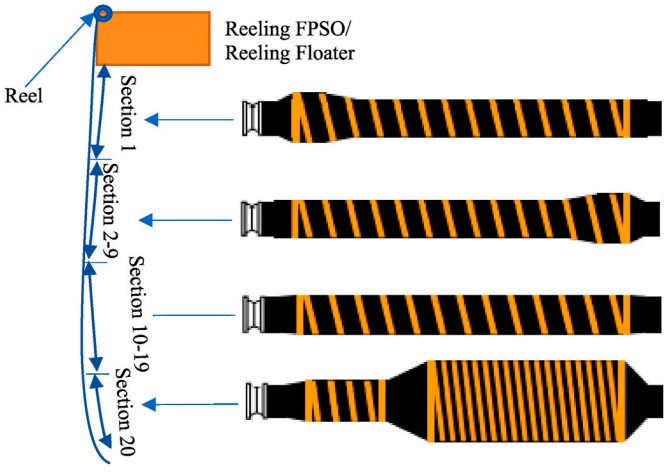

Fig. 6. An illustration showing the application of reeling hoses.

Table 7
Parameters for the reeling hose showing material properties, hose section arrangement and section detailing.

Section Number	Sub-Sections	Particulars	Inner Diameter (m)	Outer Diameter (m)	Section Length (m)	Segment Length (m)	Number of Segments	Unit Mass (kg/m)	Volume (m^3)	Segment Weight (N)
Hose Group 1:	1	H1 (Fitting)	0.489	0.650	1.0	0.325	1	495	0.330	492.5
Section 1 [first-off end with float collars]	2	H1 (Reinforced Hose End)	0.489	0.650	0.2	0.250	15	239	1.002	721.5
	3	H1 (Hose Body)	0.489	0.650	8.0	0.300	6	180	1.074	582.5
	4	H1 (Hose End)	0.489	0.675	0.5	0.300	2	200	0.320	179.0
	5	H1 (Fitting)	0.489	0.650	0.9	0.300	1	495	0.330	492.5
Hose Group 2:	6	H2 (Fitting)	0.489	0.650	0.9	0.300	1	495	0.330	492.5
Section 2—Section 9 (same) [mainline with buoyancy floats]	7	H2 (Hose End)	0.489	0.675	0.5	0.300	2	200	0.320	179.0
	8	H2 (Hose Body)	0.489	0.650	0.2	0.300	19	180	1.274	691.2
	9	H2 (Hose End)	0.489	0.675	0.5	0.300	2	200	0.320	179.0
	10	H2 (Fitting)	0.489	0.650	0.9	0.300	1	495	0.330	492.5
Hose Group 3:	11	H3 (Fitting)	0.489	0.650	0.9	0.300	1	495	0.330	492.5
Section 10—Section 19 (same) [mainline/tail line with float collars]	12	H3 (Hose End)	0.489	0.675	0.5	0.300	2	200	0.320	179.0
	13	H3 (Hose Body)	0.489	0.650	0.5	0.300	6	180	1.074	582.5
	14	H3 (Reinforced Hose End)	0.489	0.670	0.2	0.300	15	240	1.064	724.6
	15	H3 (Fitting)	0.489	0.650	0.9	0.300	1	495	0.330	492.5
Hose Group 4:	16	H4 (Fitting)	0.489	0.650	0.9	0.300	1	495	0.330	492.5
Section 20 [reinforced end buoyancy to tanker]	17	H4 (Hose End)	0.489	0.675	0.5	0.300	2	200	0.320	179.0
	18	H4 (Hose Body)	0.489	0.650	0.5	0.300	6	180	1.074	582.5
	19	H4 (Reinforced Hose End)	0.489	0.670	0.2	0.300	15	240	1.064	724.6
	20	H4 (Fitting)	0.489	0.650	0.9	0.300	3	495	0.330	492.5

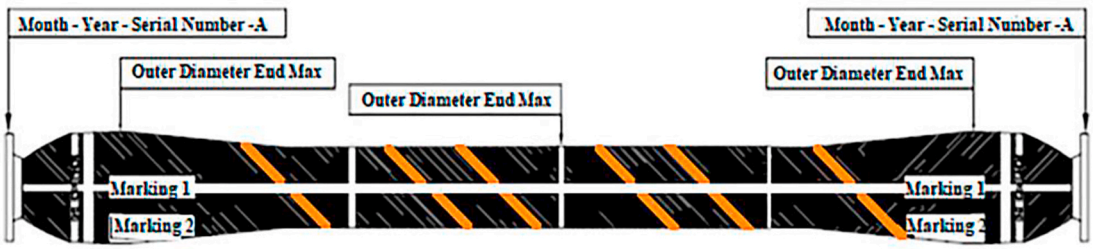

Fig. 7. Marine hose segment of 12m in length depicting markings with descriptions.

Table 8
Parameters of the cylindrical FPSO.

Parameters	Value (m)
Top diameter	56.0
Mid diameter	50.7
Base diameter	52.7
Height	50.0
Draft	20.5

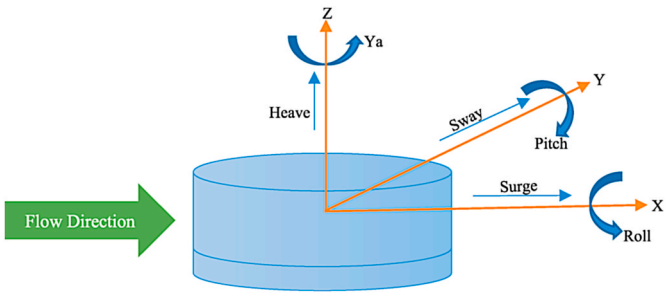

Fig. 8. Motion components showing coordinates and six degrees of freedom of a cylindrical FPSO.

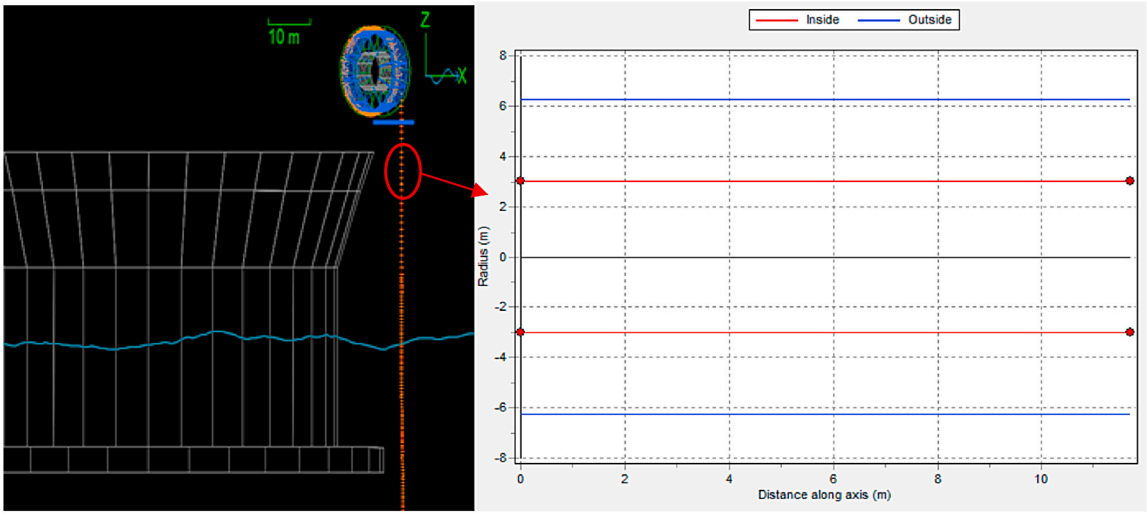

Fig. 9. FPSO-mounted reel, showing the wireframe view in Orcaflex 11.0f and profile of the reel.

Table 9
Profile for the reel.

The distance along axis (m)	Diameter (m)	Radius (m)
0.00	6.00	3.00
11.70	6.00	3.00

Table 10
Parameters for the reel.

Parameters	Value	Unit
Thickness	3.25	m
Revolution Angle	360	Deg.
Normal Stiffness	10,000	kN/m/m^2
Shear Stiffness	10,000	kN/m/m^2
Critical Damping	0.00	%

3.5. Model validation

The model was validated numerically using the results obtained from technical sources on other marine hoses [9] and experimental pipelaying sea trial tests in the open sea [47]. Some theoretical presentations and experimental works on marine hose validation are available in the literature [48,51]. On the practicality of the model, the other study on the sea trial tests [47] showed the practicality of these pipelaying designs using an S-laying configuration. However, in the present study, the hose uses both S-laying and reel-laying configurations. Thus, the numerical approach for this investigation is presented in Section 4.

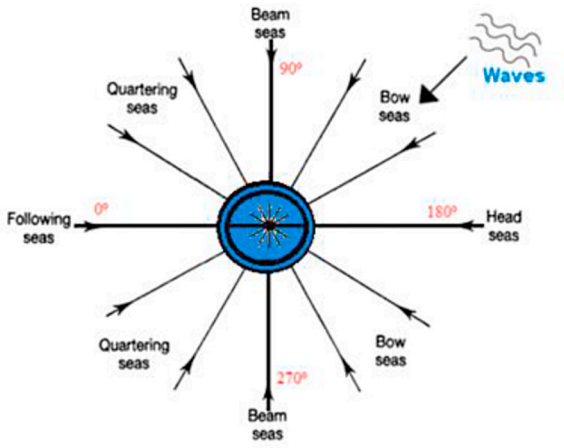

Fig. 10. Schematic of sea direction and waves on FPSOs, for the cylindrical-shaped FPSO.

4. Results and discussion

4.1. Hose response in static state analysis

In Figs. 11–13, the static state distributions for the effective tension, bending moment and curvature acting on the hose string are shown respectively. Whilst Fig. 11 shows the static state for the effective tension, Fig. 12 shows a straight profile that bends a bit which is due to the reeling nature and application of the reeling hose. This is further confirmed as it shows locations where the bending occurs closer to the start of the reeling hose (between 0m and 15m along the arc length of the hose string). From Fig. 13, the static state also reflects the nature of the curvature of the hose string for both positions. These three distributions in Figs. 11–13 also show that the results of the static state had some impact on the reeling system, which can be due to the current, winds, vessel motion, added mass, damping, and other factors. However, neglecting the effects of fluctuation in the system due to wave motion, it can be seen that the effective tension reduces along the hose string. This result is useful as it further demonstrates that the initial stage of reeling produces the highest magnitudes of tension on the structure, as well as curvature and bending, which is better illustrated by neglecting the dynamics of the wave motion. This implies that the hose ends must be well-reinforced ends with highly stiffened fittings to ensure the structural integrity of the reeling hose is maintained. As seen in Table 11, the static analysis was investigated based on three cases of the floater position, four different positions were considered and investigated. As in the plots in Figs. 11–13, Position 1 is Case 1 while Position 3 is Case 2. It can be observed that Case 1 had the maximum values for effective tension, bending moment and curvature of 879.756 kN, 34.167kNm and 0.3187, respectively, while Case 2 had the maximum values for effective tension, bending moment and curvature of 812.069 kN, 31.36kNm and 0.1532, respectively. Thus, Position 1 has the highest distribution.

4.2. Hose tension, curvature and bending moment

The strength of the hose type experiencing maximum tension and curvature was assessed against some reference hose capacity. As seen in the results of the hose strength assessment for free-hanging from the goose neck presented in Table 12, the maximum curvature of 0.499 was observed in load Case 2, while the maximum tension of 1,088 kN was observed in load Case 1. The result presented showed that this type of hose is very suitable for this reeling application, as the maximum tension observed is below the allowable tension for both load cases. The free-hanging reeling hose was considered in this study, as depicted earlier in Fig. 9. The study was considered in the study on the load response of the reeling hose, as presented in Figs. 14–16. The hose behaviour has shown that the effective tension was maximum at the end that is attached to the reeling vessel. Also, the load response on the reeling hose shows that

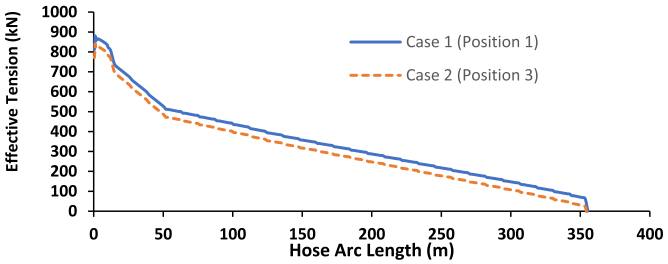

Fig. 11. Static state effective tension of the reeling hose for Position 3.

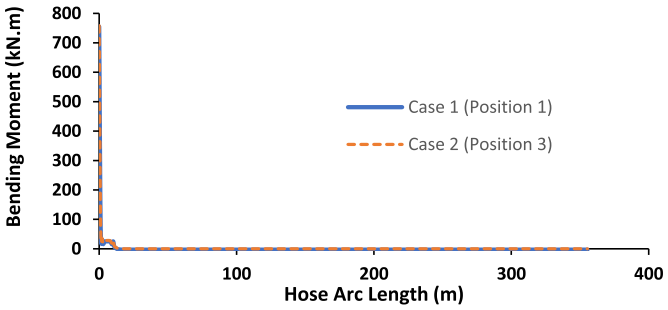

Fig. 12. Static state bending moment of the reeling hose for Position 3.

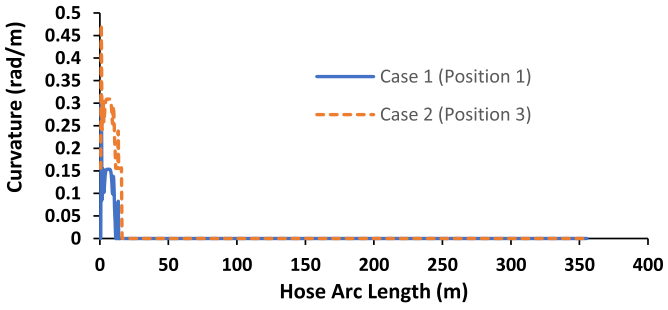

Fig. 13. Static state curvature of the reeling hose for Position 3.

Table 11
Result of the static analysis of the reeling hose.

FPSO Position	Maximum Bending Moment (kNm)	Maximum Effective Tension (kN)	Maximum Curvature (1/m)
Position 1	**34.167***	**879.756***	**0.3187***
Position 2	32.64	878.012	0.1734
Position 3	31.36	812.069	0.1532
Position 4	30.42	805.810	0.1314

Table 12
Hose strength assessment for free hanging reeling hose.

Load Case	Description	Hose Type	Maximum Tension (kN)	Maximum Curvature (1/m)	Allowable Tension (kN
Case 1	Hs = 5.5m, Tp = 14s, curr. = 0.6m	Reinforced	**1088***	0.393	**2493**
Case 2	Hs = 5.5m, Tp = 16s, curr. = 0.6m		1085	**0.499***	**1970**

as it reels, the curvature of the hose also shows that the embedded floats inside the hose also lead to the stresses on the reeling hoses. In Fig. 14, the bending moment is reduced to capture up to 200kNm, and the bending moment distribution along the arc length appears to be undulating, due to the connections attached to the hose at the hose ends. The maximum curvature of the hose in Fig. 15 is less than 1 rad/m, at 0.5 rad/m which shows it is fit for use, according to OCIMF [40]. From the selected profiles, the maximum effective tension obtained is 894 kN as in Fig. 16. It can be concluded that the ends of the hoses need to be highly reinforced as the tensions between 0 and 15m are high. However, it will be necessary to further investigate the stresses in those sections.

4.3. Hose bending strain, tensile strain and pipelay strain

In this section, the strain of the marine bonded hoses is assessed using three different parameters – the maximum bending strain, the direct tensile strain and the pipelay strain. Presently, the specification in the industry standard DNV-ST-F101 [52], suggests assessing the strain during reeling by considering Accumulated Plastic Strain (APS) which is recommended at 2 %, but this can increase due to the limitation of plastic deformation on the bonded hose materials selected. However, this study proposes other methods of assessing strain with the proposed limits. As observed in Figs. 17–19, the strain profiles are presented for minimum, mean, maximum and standard deviation profiles. The profile distribution for the free-hanging mode of the hose string from the goose neck shows the maximum bending strain, direct tensile strain and pipe-lay von Mises strain. A commonality observed in these distributions is that the

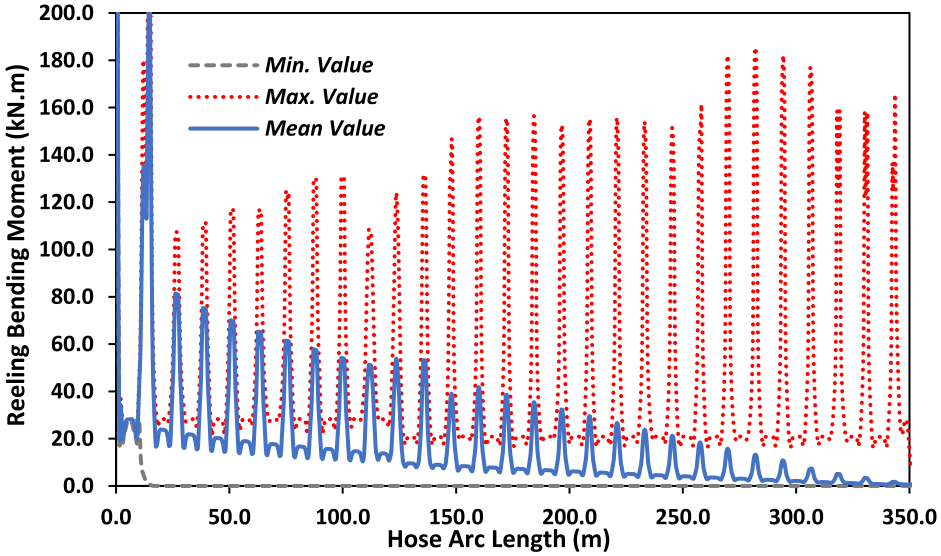

Fig. 14. Results of the bending moment for the free-hanging mode from the goose-neck.

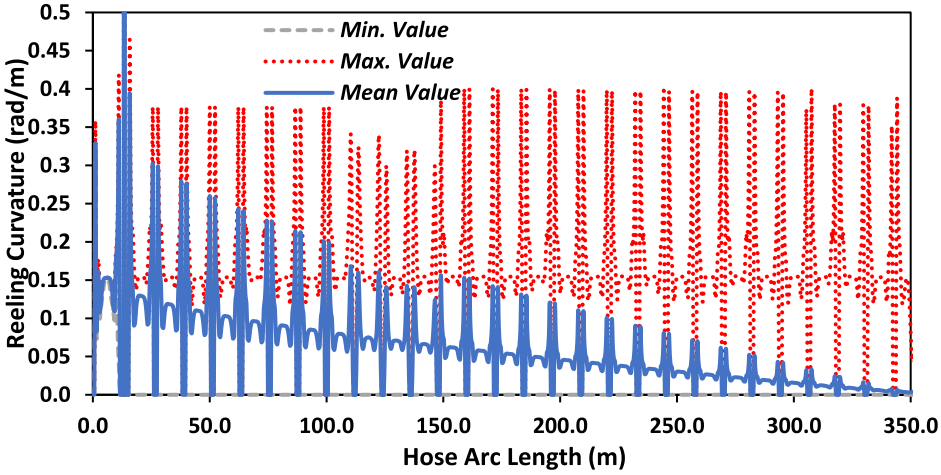

Fig. 15. Results of the curvature for the free-hanging mode from the goose-neck.

maximum value has the highest distribution, followed by the mean distribution and the least is the minimum value, as in Figs. 17–19. In Fig. 17, the profile distribution for the direct tensile strain across the arc length of the hose is observed to be in regular amplitudes generated after each hose section length at points where there are end-connections, hose couplings and hose fittings, however, the profile has three phases. The first phase of amplitudes with direct tensile strains is from 1.04 % to 0.78 % for arc lengths 0m–125m, while the second phase of amplitudes is observed across arc lengths 126m–340m with direct tensile strains from 1.27 % to 0.45 %. The third phase goes from the arc length of 341m to the end of the arc length with a direct tensile strain starting at 0.24 %. In Fig. 18, the maximum direct tensile strain is 1.27 % while the mean tensile bending strain is 0.81 %. In Fig. 19, the profile of the maximum bending strain has an amplitude that was generated after each hose section length, as such at points where there are end-connections, hose couplings and hose fittings, the bending strains are very minimal. This appears to be quite consistent throughout the hose string from this investigation. The maximum bending strain was 5.53 % while the mean bending strain was 1.36 % from the averaged mean value. The profile of the pipelay von Mises strain has an amplitude that was also generated after each hose section length at points where there are end-connections, hose fittings and hose couplings. These could include end-fittings, Marine Breakaway Couplings (MBC) and Hose End Valves (HEV). The pipelay von Mises strains were used to assess the hose strain during pipelaying of the reeling hose from a pep-laying or reel-mounted FPSO. From this investigation, pipelay von Mises strains were very minimal and within the safe limits for use with an average of 15.8 %. However, towards the end of the hose string, the pipelay von Mises strain increased to 26 % due to the tensioner holding it on the stringer while the hose string is hose-lay, depending on the chosen hose configuration. As can be seen in Fig. 19, there are three phases with maximum pipelay von Mises strains of 4 %, 6.34 % and 15.8 %, while the mean pipelay von Mises

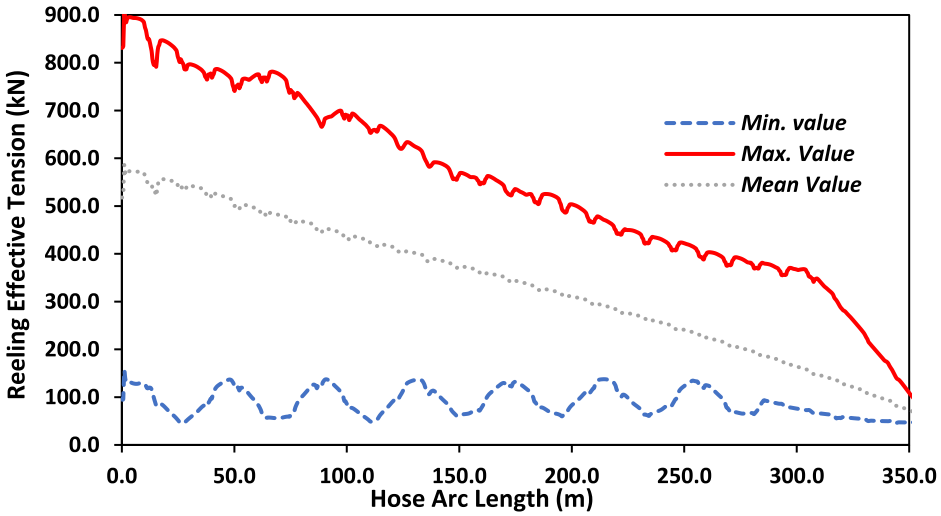

Fig. 16. Results of the effective tension for the free-hanging mode from the goose-neck.

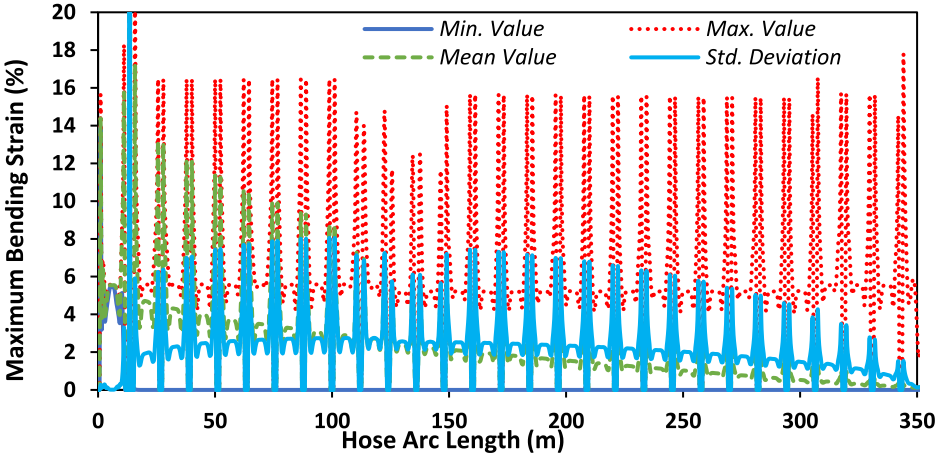

Fig. 17. Results of the maximum bending strain for the free-hanging mode from the goose-neck.

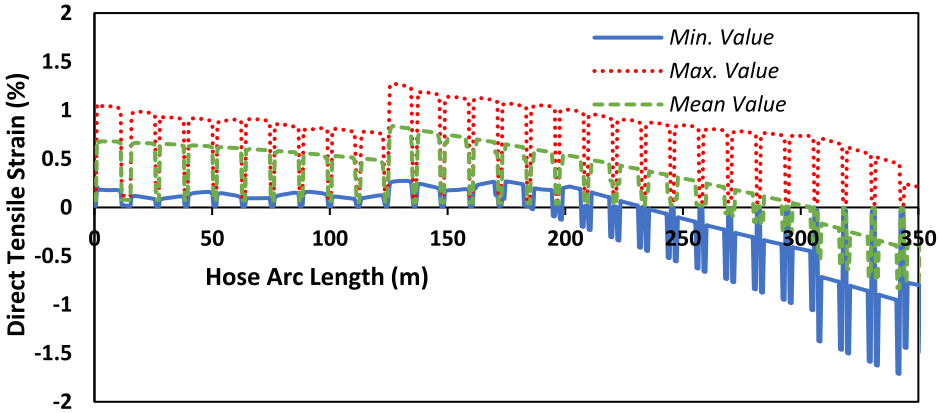

Fig. 18. Results of the direct tensile strain for the free-hanging mode from the goose-neck.

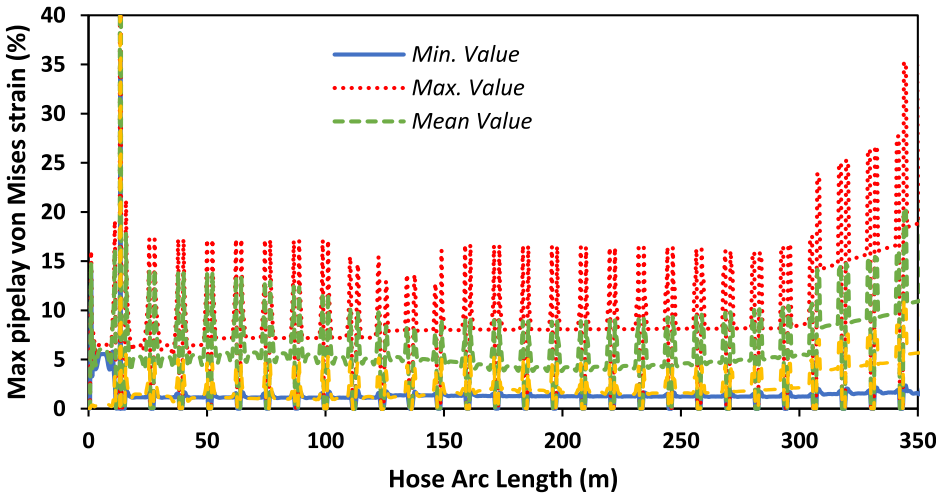

Fig. 19. Results of the pipelay von Mises strain for the free-hanging mode from the goose-neck.

strain is 0.02 %, 1.52 % and 5.27 %. Thus, it can be observed that these strain values have different profiles, but the strains are close to that of the Accumulated Plastic Strain (APS) of 2 % in the industry standard DNV-ST-F101 [52], and the variances are within close limits of satisfaction. This also shows good agreement that these methods of strain assessments can be considered in the design of marine bonded hoses, however, APS considers the total principal strains. In Fig. 19, the pipelay von Mises strain had the widest margin of variance. This could also indicate the behaviour of the material, or material properties used for the calculation considered in the von Mises strain, but it shows profiles of the strained and unstrained regions. Due to the locus of the yield stress on the hose section being reeled, the hose material had a plastic behaviour that was observed after reeling. As such, these three methods of assessing strains are considered to show good agreement. It is noteworthy to state that the reel-laying subjects the pipeline to large bending which induces plastic strain reversals as the pipeline is reeled on and off followed by aligning and straightening before exiting the installation vessel as also seen in this study [20,21,53].

4.4. Hose shear force, stress and strength

The shear force, maximum bending stress and the von Mises stress of the free-hanging reeling hose were conducted in the current study, as presented respectively in Figs. 20–22. Shear force showed that the distribution along the arc length presents a uniform distribution on the load response of the reeling hose, as presented in Fig. 20. As observed, the shear force shows a pattern of several hose segments under the free-hanging position, which implies that the hose elements along the plane act in the same direction but deviate to another plane to also give a higher shear force along the hose arc length. However, for the maximum bending stress, the distribution is based on the fatigue it experiences as it appears to be circumferential stress showing a similar hysteresis behaviour noticed during hose fatigue on a Mohr's circle, however, it is subject to further fatigue study on the hose. In addition, the maximum bending stress appears to increase along the hose string profile as it tends towards the end, as shown in Fig. 21. In Fig. 22, it is evident that the von Mises stress reduces along the arc length until it reaches close to 257m arc length and then it spikes up. This shows that the hose reinforcement can be affected by the stiffness of the end-fittings on each of the hose segments.

4.5. Strength assessment of reinforced and mainline hoses

The assessment of the hose strength was conducted for two types of hoses - the reinforced hose and the mainline hose types, as presented in Table 13. Critical load combinations were used for 1000 years of storm conditions. The tabulated results show that the hose performed well under freshwater and seawater test conditions. It can be observed that the reinforced hose has a higher distribution than the mainline hose distribution in both the 0° and 90° wave headings. In addition, the seawater profile is higher than the freshwater profiles, as observed in Table 13. Also, the hose profiles observed were maximum under the reinforced hose type in 0° wave heading with a tension of 1,557 kN and an allowable tension of 4199 kN under the seawater condition, while the least was the mainline hose type in 90° wave heading with a tension of 952 kN and an allowable tension of 3418 kN under the freshwater condition. Thus, it can be confirmed that the hose is fit for use as designed and that the strength of the hose is of good capacity. The assessment conducted on the hose strength and critical load combination showed satisfactory performance. However, it also shows notable differences in the profiles for the two scenarios because the hose string was designed according to the environmental demand, and the hose type required to ensure that it can deliver the required usage in testing, application and operation. However, further work is required on each section of the reeling hose with respect to the connections.

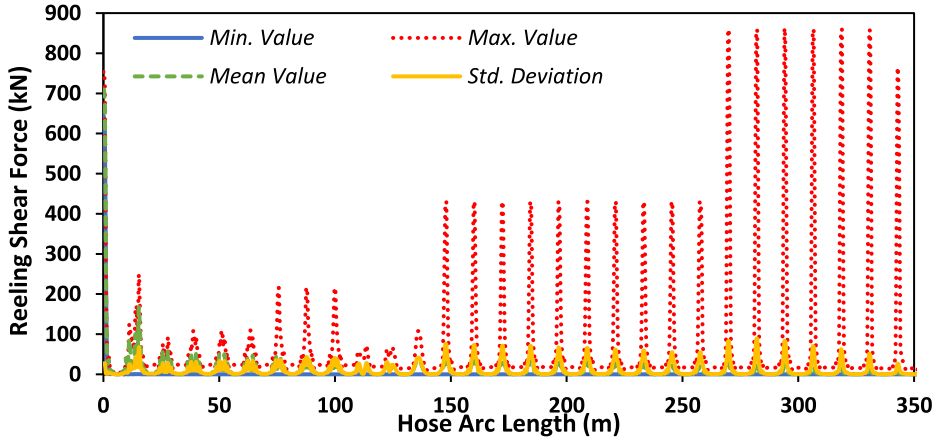

Fig. 20. Result of the shear force for the free-hanging mode from the goose-neck.

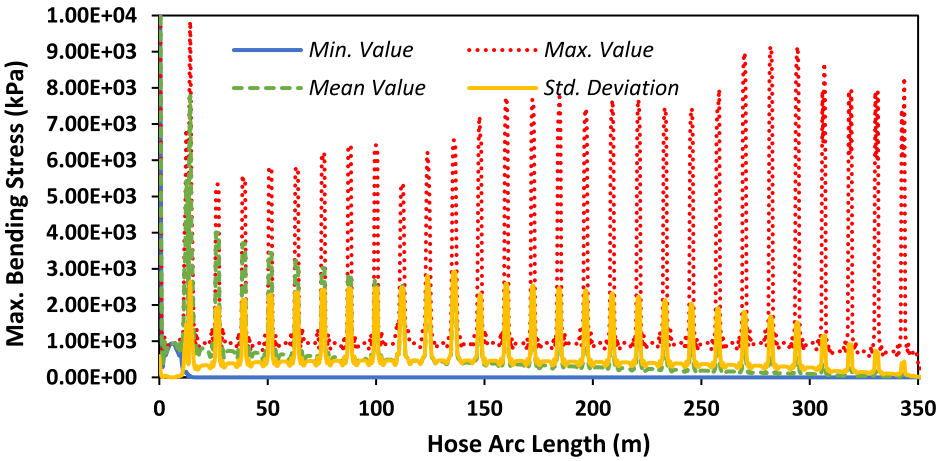

Fig. 21. Result of the max. bending stress for the free-hanging mode from the goose-neck.

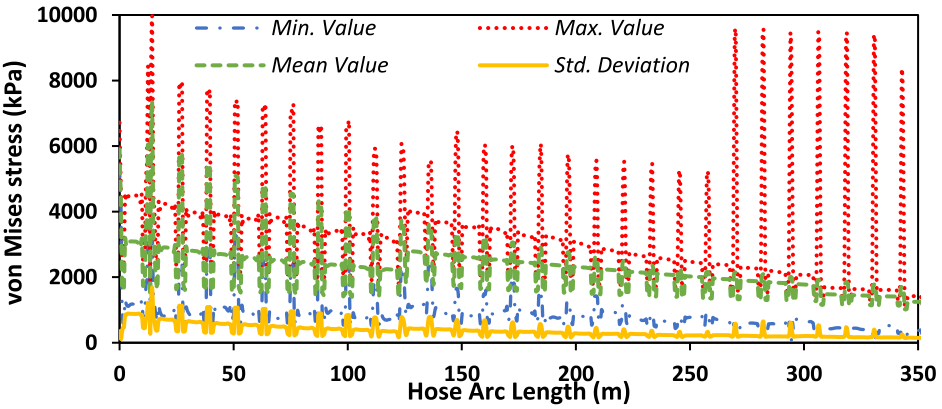

Fig. 22. Result of the von Mises stress for the free-hanging mode from the goose-neck.

Table 13
Assessing the strength of two hose types from critical load combination.

Content of Hose	Fluid Content Density	Wave Heading Angles	Type of Hose	Max. Eff. Tension (kN)	Max. Curvature (1/m)	Allowable Tension (kN)
Seawater	1,025 kg/m^3	0°	Reinforced	1557	0.125	**4199**
			Mainline	1114	0.013	**3418**
		90°	Reinforced	1409	0.059	**4118**
			Mainline	961	0.011	**3418**
Freshwater	1,000 kg/m^3	0°	Reinforced	1528	0.131	**4036**
			Mainline	1109	0.013	**3418**
		90°	Reinforced	1374	0.059	**4117**
			Mainline	952	0.011	**3418**

4.6. Effect of fluid contents on free-hanging hose

The effect of fluid contents on free-hanging reeling hose was investigated using freshwater and seawater of densities 1000 kg/m^3 and 1025 kg/m^3, respectively. This was conducted under survival conditions, as presented in Table 14. The analysis for the survival study was carried out using wave data for a 100-year return period and 1 year and current data. The hose design was conducted, as specified in OCIMF [40], and API 17K [39]. In the static analysis as presented in Table 15, it was observed that the second case (Case 2 which is the seawater) had the highest tension, with a maximum tension of 764 kN, while the freshwater has a maximum tension of 751 kN. Thus, the denser the fluid content in the hose, the higher the tension. In the dynamic analysis in Table 16, a higher environmental condition with 4 wave headings was considered, and it was observed that the maximum tension of 1496.0 kN was observed under seawater content, while the maximum bending of 70.44 kNm and maximum curvature of 0.131 rad/m were observed under freshwater content. It was conducted using four sea types for the wave heading: the following sea (0°), the beam seas (90° and 180°) and the head sea (270°), as depicted earlier in Fig. 10. The wave headings affected the hose parameters and the fluid contents. It can be deduced that the seawater influenced the effective tension more while the freshwater influenced the maximum bending moment and curvature more. However, this is relative and depends on the angle of the wave heading. The hose types also showed satisfactory performance for 100 years of storm condition. Lastly, the ball-joint connection from the hang-off table showed that the connection stiffness is 2.33 kNm/deg, as illustrated in Fig. 23.

4.7. Effect of wave heading angles on free-hanging hose

The effect of the wave heading angles was also investigated on the free-hanging hose types, as presented in Table 17 and Figs. 24–26. From Tables 17 and it can be observed that the maximum effective tension was 930.4683 kN which was observed at 90° wave heading. Also, the maximum bending moment was 64.5784kNm which was observed at 45° wave heading while the maximum curvature was 0.4589 which was observed at 30° wave heading. This shows that different wave headings have different effects on the hose string. It is further supported by the plots in Figs. 24–26, however, it is evident that it occurs in phases. For the effective tension from Fig. 24(b), the magnitude of the phase interval is 45° > 0° > 90°, while in Fig. 24(c), the magnitude of the phase interval is 45° > 30° >15° and in Fig. 25(d), the magnitude of the phase interval is 60° > 75° > 60°. This confirms that there is a pattern in the hose response for effective tension. For the bending moment from Fig. 26(b), the magnitude of the phase interval is 0° > 45° > 90°, while in Fig. 25(c), the magnitude of the phase interval is 15° > 30° > 45° and in Fig. 25(d), the magnitude of the phase interval is 90° > 75° > 60°. This confirms that there is a pattern in the hose response concerning the bending moment. For the curvature from Fig. 27(b), the magnitude of the phase interval is 90° > 45° > 0°, while in Fig. 26(c), the magnitude of the phase interval is 15° > 30° > 45° and in Fig. 26(d), the magnitude of the phase interval is 90° > 75° > 60°. This confirms that there is a pattern in the hose response for curvature. Thus, it can be concluded that the wave heading angle influences the load response of the hose, relative to the segment of the hose.

Table 14
Design conditions under survival conditions with different fluid contents.

Design Conditions	Descriptions
Condition 1	A parametric study using different hose models was conducted for survival conditions in 100 years of storm
Condition 2	Hanging from the hang-off table (straight from the table through keel downwards)
Condition 3	Hose string is unpressurized; 0 bar
Condition 4	Processed water or fresh water and seawater filled; (1,000 kg/m^3 and 1,025 kg/m^3)
Condition 5	A connection stiffness of 2.33 kN m/deg was used at the ball-joint connection
Condition 6	The effect of wave headings was investigated at 0°, 90°, 180° and 270°
Condition 7	The analysis for the survival study was carried out using wave data for a 100-year return period and 1 year and current data. Specifications used: OCIMF [40], and API 17K [39]

Table 15
Results for static analysis on the free-hanging hose.

FPSO Draft	Hose Content	Cases	Maximum Tension (kN)	Maximum Bending (KNm)	Maximum Curvature (1/m)
Ballast	Freshwater 1,000 kg/m^3	Case 1	751.0	0.0	0.0
	Sea water (1,025 kg/m^3)	Case 2	764.0	0.0	0.0

Table 16
Results of the dynamic analysis on Hose string load combination for 100-year storm conditions.

Hs (m)	Tp (s)	Hose Content	Wave Headings	FPSO Draft	Max. Ten. (kN)	Max. Bend. (KNm)	Max. Curv. (1/m)
13.5	15.7	Freshwater (1,000 kg/m^3)	0°	Ballast	1561.0	**70.44**	**0.131**
			90°		1411.0	53.71	0.063
			180°		1358.0	40.62	0.048
			270°		1323.0	43.53	0.053
		Seawater (1,025 kg/m^3)	0°		**1496.0**	69.42	0.128
			90°		1430.0	53.51	0.061
			180°		1370.0	40.43	0.045
			270°		1341.0	45.24	0.052

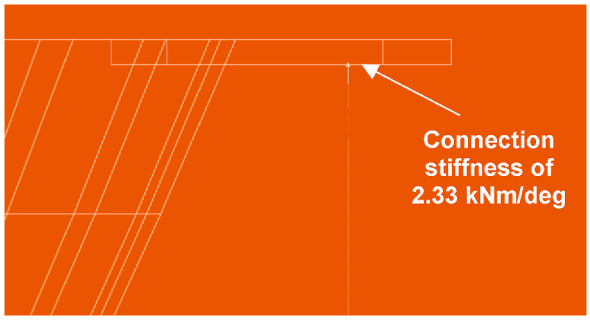

Fig. 23. Ball-joint connection from hang-off table showing connection stiffness.

Table 17
Result summary of maximum effective tension, maximum bending moment and maximum curvature.

Wave Angle	0°	15°	30°	45°	60°	75°	90°	Max Values
Max. ET	918.6108	910.5366	910.2748	921.0894	914.8686	915.4551	930.4683	930.4683
Max. BM	61.5954	60.6697	60.5389	64.5784	61.6369	62.0345	62.4175	64.5784
Max. Curv.	0.457646	0.457709	0.458869	0.457338	0.458185	0.457711	0.45771	0.458869

4.8. Effect of current speed on free-hanging hose

For the free-hanging hose, as represented in Fig. 27, the results of the maximum load combinations of the hose string were obtained for the dynamic analysis for two different current cases, as presented in Table 18. In the first case under Hs of 5.6m, Tp of 16s and current speed of 0.0 m/s, the maximum tension was 1,078 kN, while the maximum bending moment was 92.1kNm and the maximum curvature was 0.395. In the second case under Hs of 5.6m, Tp of 16s and current speed of 0.55 m/s, the maximum tension was 1,089 kN, while the maximum bending moment was 91.80kNm and the maximum curvature was 0.398. These values show that the hose was fit for reeling operation. It can be concluded that the current speed influences the hose string as higher currents present higher effective tensions, bending moments and curvature values. The free-hanging reeling hose string showing the section of the reeling hose having the maximum tension is depicted in Fig. 27.

4.9. Effect of simulation time steps and CPU clock on hose model

A parametric study was conducted on the influence of simulation time on the reeling hose model, using six cases, having time steps 0.1s, 0.01s, and 0.001s and two wave headings at 75° and 90°. In Fig. 28, it can be observed that the 90° wave headings had higher effective tensions than the 75° in all cases. This implies that the higher the wave angle, the higher the effective tension. In Figs. 29 and 30, it can be observed that the 90° wave headings had higher bending moment and curvature than the 75°, however, not in all cases. The pattern shows that [t = 0.001s, θ = 90°] > [t = 0.001s, θ = 75°] > [t = 0.01s, θ = 90°] > [t = 0.01s, θ = 75°] > [t = 0.1s, θ = 90°

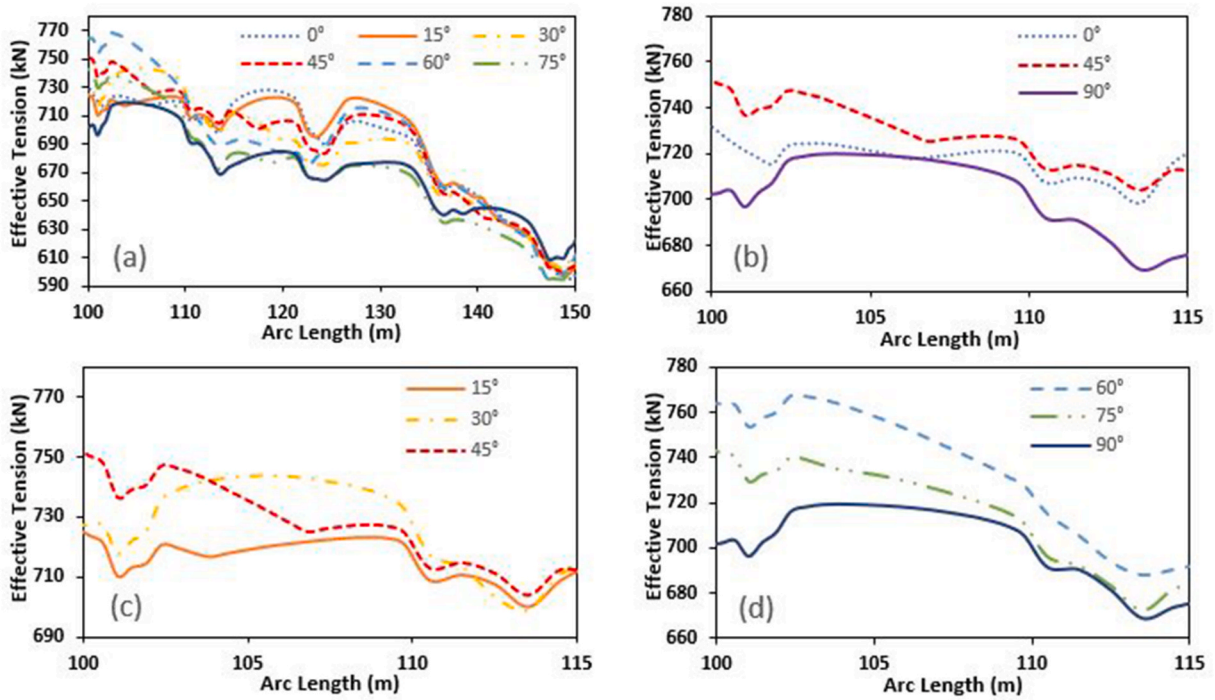

Fig. 24. Result of the hose effective tension under different simulation runs: (a) 0°,15°,30°,45°,60°, 75°;(b) 0°,45°, 90°; (c) 15°,30°, 45°; and (d) 60°,75°,90°.

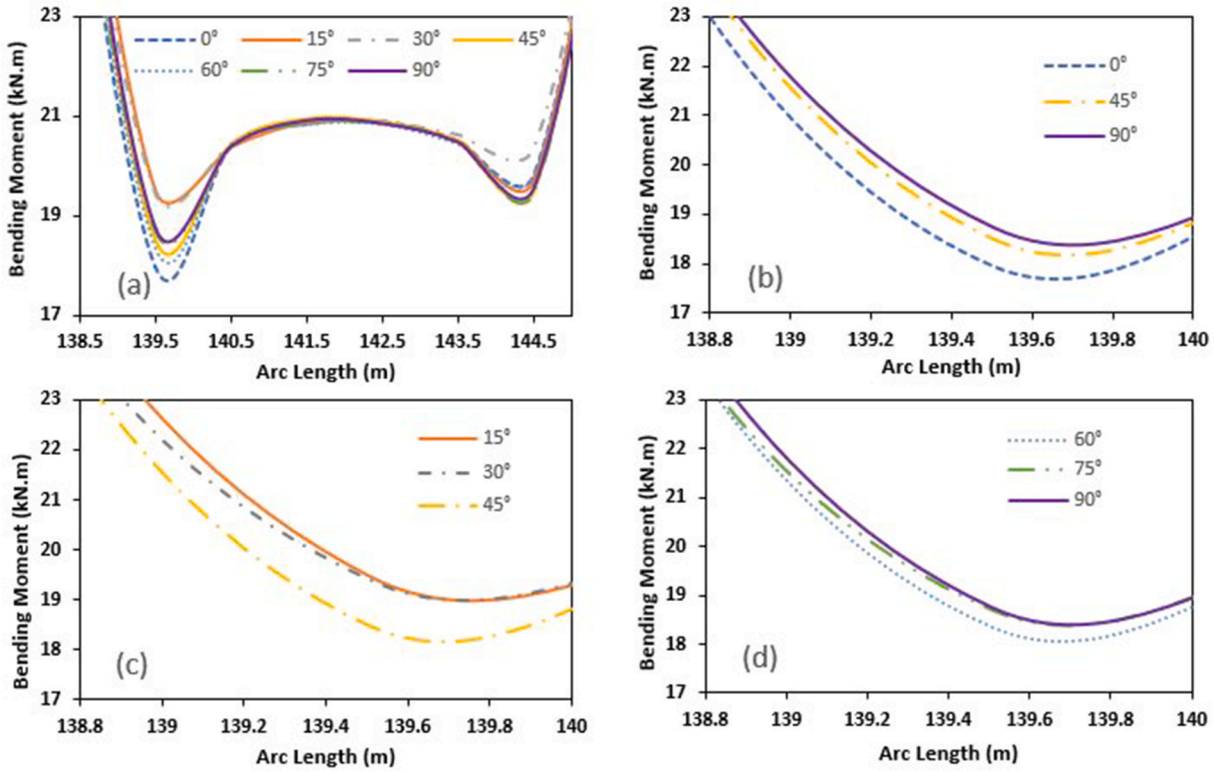

Fig. 25. Result of the hose bending moment under different simulation runs: (a) 0°,15°,30°,45°,60°, 75°; (b) 0°,45°, 90°; (c) 15°,30°, 45°; and (d) 60°,75°,90°.

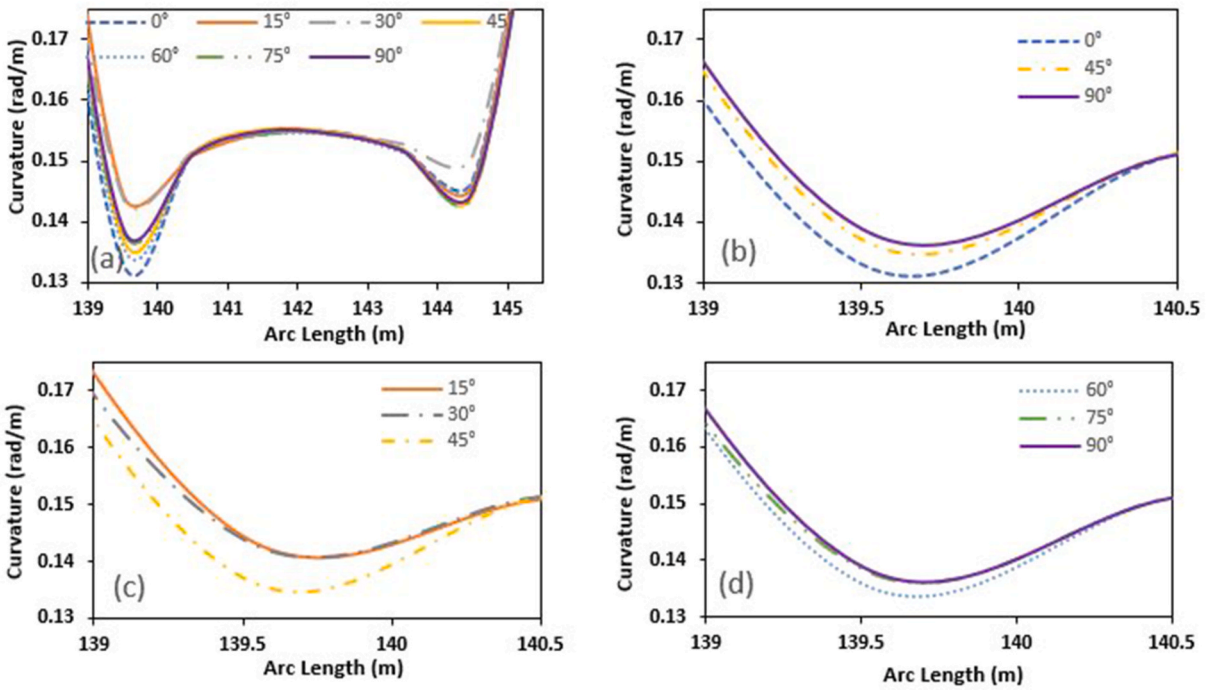

Fig. 26. Result of the hose curvature under different simulation runs: (a) 0°,15°,30°,45°,60°, 75°; (b) 0°,45°, 90°; (c) 15°,30°, 45°; and (d) 60°,75°,90°.

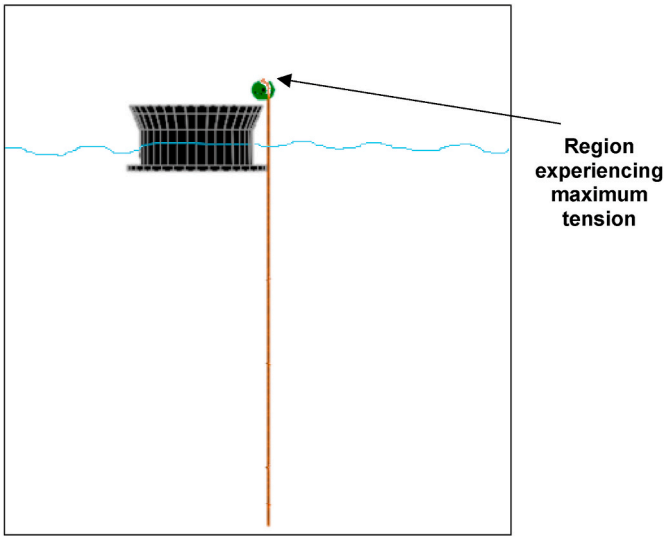

Fig. 27. The free-hanging reeling hose string showing the section of reeling hose having max. bending and max. tension.

] > [t = 0.1s, θ = 75°]. This implies that the higher the wave angle, the higher the bending moment and curvature. Thus, the simulation time steps influence the hose model. It should be noted that for smaller time steps of 0.0001s, the amount of data generated during the dynamic simulation time series was quite large but was able to work within the capacity of the Orcaflex's software working memory using supercomputers and workstations. The maximum effective tension has a good agreement for the time steps 0.1s, 0.001s and 0.0001s, which validates the model, especially as the simulations are usually unstable under very high-stress values at the top end of the hoses. Since the 0.1s is faster, and also more stable, it was chosen for the model.

An additional parametric study on the effect of simulation timestep on the hose model is carried out using different simulation timesteps, as presented in Figs. 31–33. CPU run time was related to the number of degrees of freedom of the input model. The model used for the CPU run time study was a reeling hose model attached to the FPSO. It can be observed in Fig. 31 that the higher the CPU

Table 18
Maximum load combinations on hose string in dynamic analysis.

Hs (m)	Tp (s)	Max. Ten. (kN)	Max. Bend. (kNm)	Max. Curv. (1/m)	Max. Ten. (kN)	Max. Bend. (kNm)	Max. Curv. (1/m)
		0.0 m/s current speed			0.55 m/s current speed		
5.6	8	1046.0	92.00	0.395	1048.0	91.50	0.393
	10	1047.0	92.00	0.395	1052.0	91.60	0.393
	12	1050.0	92.00	0.395	1061.0	91.70	0.393
	14	1055.0	92.00	0.395	1078.0	91.70	0.393
	15	1076.0	92.00	0.395	1085.0	91.70	0.393
	16	1078.0	92.10	0.395	**1089.0***	**91.80***	**0.398***

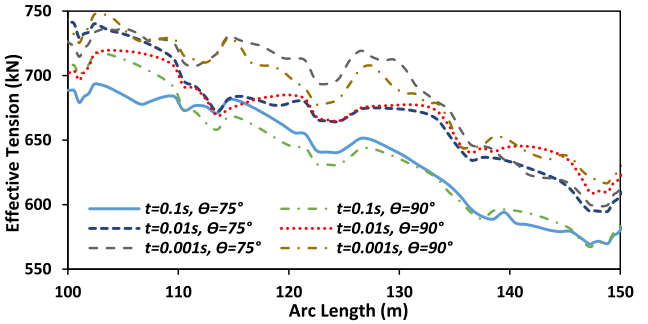

Fig. 28. Results of the hose effective tension under different simulation time steps: (a) t = 0.1s, θ = 75°; (b) t = 0.01s, θ = 75°; (c) t = 0.001s, θ = 75°; (d) t = 0.1s, θ = 90°; (e) t = 0.01s, θ = 90°; and (f) t = 0.001s, θ = 90°.

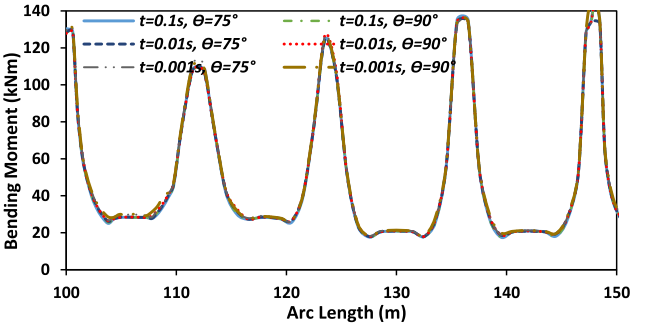

Fig. 29. Results of the hose bending moment under different simulation time steps: (a) t = 0.1s, $\theta = 75°$; (b) t = 0.01s, $\theta = 75°$; (c) t = 0.001s, $\theta = 75°$; (d) t = 0.1s, $\theta = 90°$; (e) t = 0.01s, $\theta = 90°$; and (f) t = 0.001s, $\theta = 90°$.

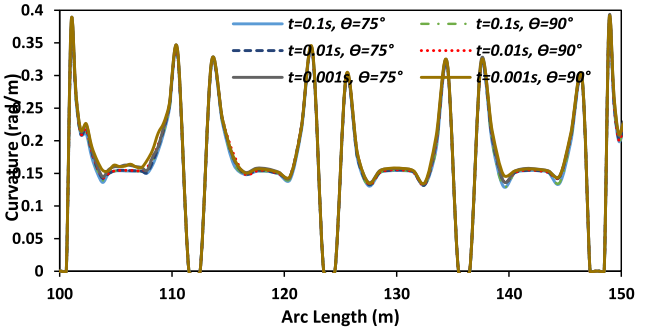

Fig. 30. Results of the hose curvature under different simulation timesteps: (a) t = 0.1s, $\theta = 75°$; (b) t = 0.01s, $\theta = 75°$; (c) t = 0.001s, $\theta = 75°$; (d) t = 0.1s, $\theta = 90°$; (e) t = 0.01s, $\theta = 90°$; and (f) t = 0.001s, $\theta = 90°$.

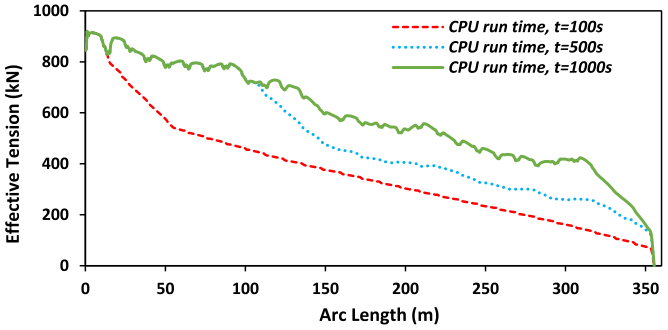

Fig. 31. Plot on hose effective tension under different CPU run times: (a) 100s; (b) 500s; and (c) 1000s.

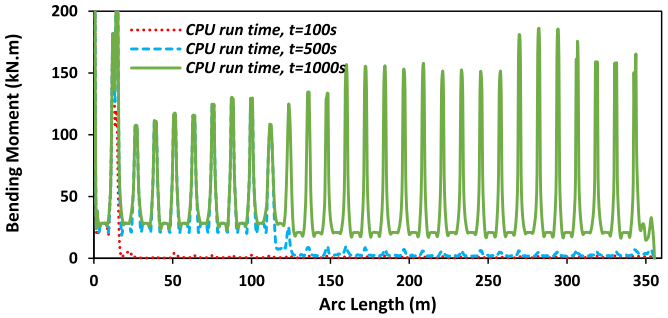

Fig. 32. Plot on hose bending moment under different CPU run times: (a) 100s; (b) 500s; and (c) 1000s.

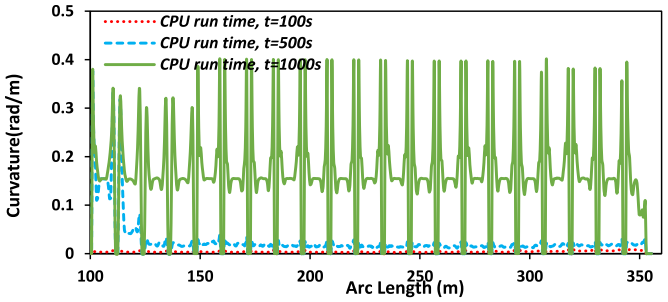

Fig. 33. Plot on hose curvature under different CPU run times: (a) 100s; (b) 500s; and (c) 1000s.

run time, the higher the effective tension. At CPU run time, t = 1000s, the maximum effective tension profile was obtained, followed by the CPU run time, t = 500s and the least is the CPU run time, t = 100s. Thus, more data were captured in the first case with CPU run time, t = 1000s. This validates the study and confirms that the model is in good agreement. In Figs. 32 and 33, similar trends are also observed as CPU run time, t = 1000s has the highest profile of bending moment and curvature. Thus, the simulation run time influences the hose model and can be considered a major variable in validating similar hose models numerically.

4.10. Effect of solid contact on hose model

The initial stage of the riser reeling process is important for close observation as it demonstrates the maximum potential for riser fatigue and ultimate failure of the structure. The region of the reeling hose model that was identified to have highest bending and tension can be seen in Fig. 34. However, due to the weight of the connection ends and HEVs, there is solid contact made from the extra load. Thus, we also loaked at the hose-string contact force as seen in the solid contact time series in Fig. 35. This time series shows that while the amplitude of the solid contact force concerning time is constant, the wavelength decreases. It was also observed that the solid contatc for the reeling hose, as shown in Fig. 36, shows that the hose's solid contact force profile is distributed along the arc lengths. For the solid force, it was recorded that contact was made at: 273.650 (kN/m) at 1.50m.

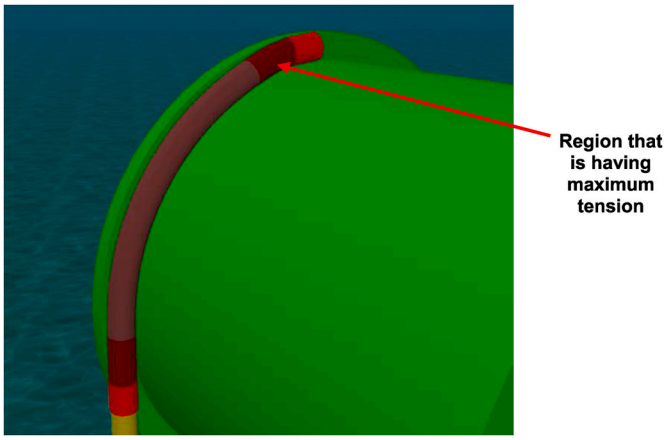

Fig. 34. Region that is having maximum tension and bending.

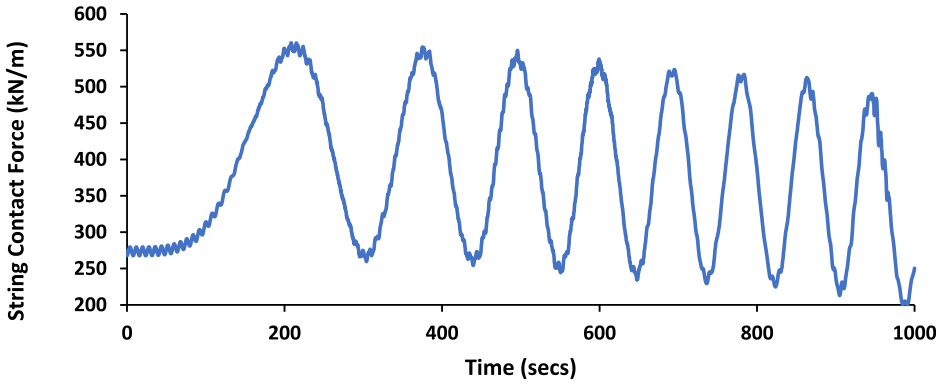

Fig. 35. Time series of the solid contact force for the marine reeling hose.

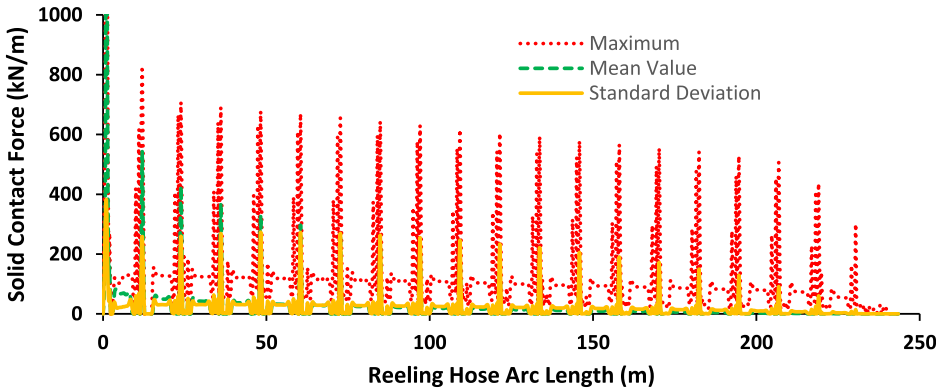

Fig. 36. *Reeling hose solid contact force,* for the arc length 0–250 cm.

4.11. Effect of fluid content density on hose model

The reeling hose was investigated for its behaviour under different fluid contents, by using internal contents of seawater, crude oil and nitrogen gas. Each fluid had a different natural density than the others, therefore the resulting mechanical data were different. Different densities incur different magnitudes of internal pressure inside the hose line. The internal force being applied to the inside face of the hose line affects the mechanical behaviour of the pipeline during the reeling process. The same simulation used to obtain the initial results was also used to obtain the results for different internal fluid transport. As seen in Figs. 37–39, it can be demonstrated that the density of fluids has a significant effect on mechanical data during the reeling process. Seawater, being the densest fluid,

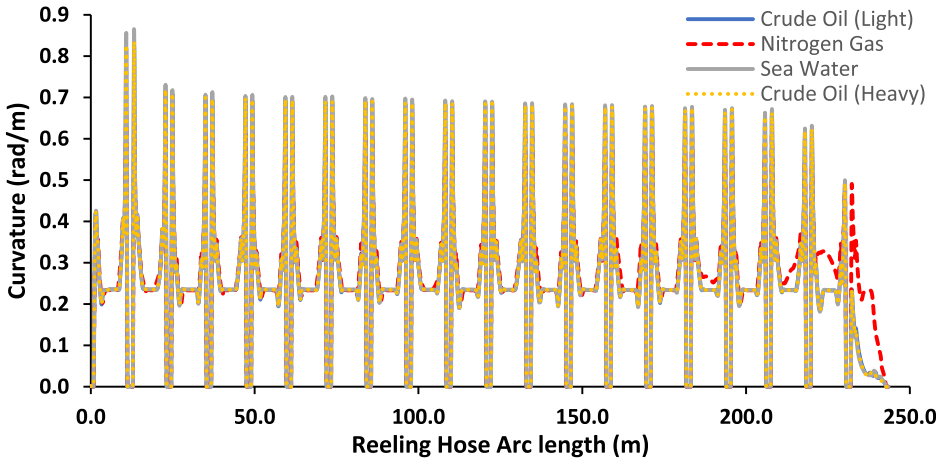

Fig. 37. Reeling hose comparative result for hose curvature using different fluid contents namely: (a) crude oil-light density; (b) nitrogen gas; (c) sea water; and (d) crude oil-heavy density.

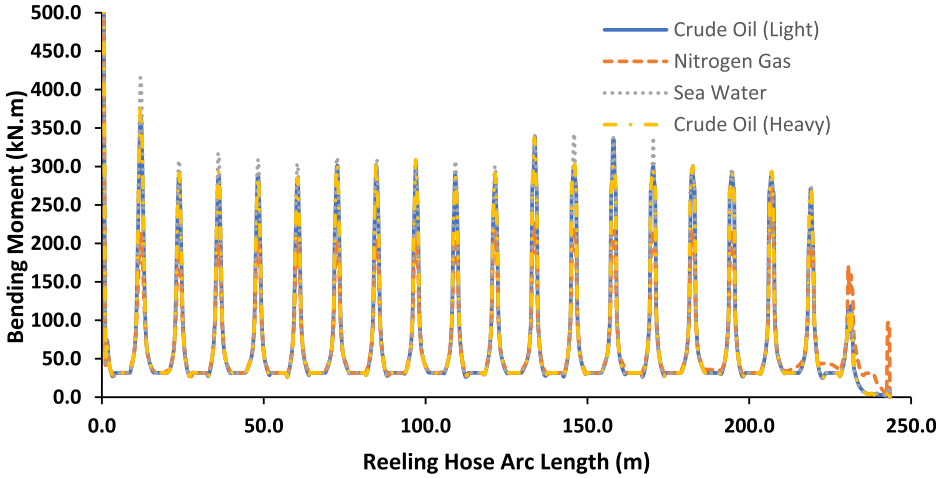

Fig. 38. Reeling hose comparative result for bending moment using different fluid contents namely:(a) crude oil-light density*;* (b) nitrogen gas, (c) *sea water;* and (d) crude oil-heavy density.

demonstrates an increase of around 350 kN/m compared to that of nitrogen gas, with crude oil producing results just below the results trend for seawater. With regards to curvature, again seawater demonstrates the largest magnitudes of curvature change of the pipeline as the reeling process progresses, with nitrogen gas and crude oil following the same trend closely. Finally, the repeating trend observed on the bending moment distribution continues with the notion that seawater content produces the highest magnitude of bending moment throughout the structure, closely followed by crude oil and nitrogen gas. However, as an important observation, it can be observed that nitrogen gas results, in comparison to the other transport fluids, produce the highest magnitude of result for all cases (curvature, bending moment and effective tension) in the final stages nearing reeling completion. As an overall observation, it can be confirmed that the density of fluid undoubtedly influences the mechanical behaviour of the pipeline, as the increased weight adds increased amounts of force to the pipeline structure. Fluctuations in results are, again, caused by variations in wave motion as the pipeline slightly sways as the reeling process occurs, this introduces an element of cyclic loading of the structure, suggesting a likely source of fatigue on the pipeline structure itself.

4.12. Discussion

This section presents a discussion of the results of the load response and the parametric studies of the reeling hose. In this study, the global design was conducted under different environmental sea states and two wave spectra. Different industry guidelines have been utilised in the modelling and design of the offshore structures [50,52,54,56,65,67–70]. From the global design analysis, the results obtained in this study provide valuable findings for understanding the fundamental load response and strain-wise mechanical behaviour during both operational and static non-operational conditions and reeling operations. This is important because the marine

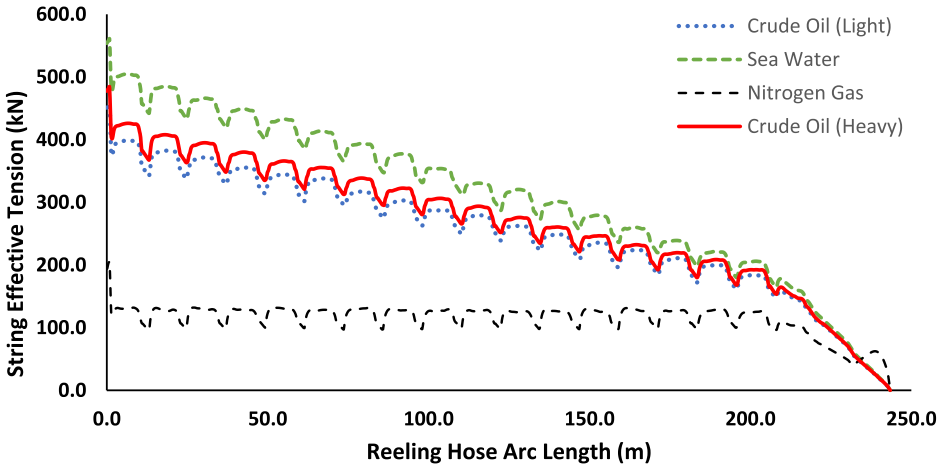

Fig. 39. Reeling hose comparative result for effective tension using different fluid contents namely:(a) crude oil-light density; (b) nitrogen gas*; (c) sea water; and* (d) crude oil-heavy density.

bonded hose is designed for a reeling system mounted on a cylindrical FPSO, but the approach could be applied to other operations. However, further research is recommended on this investigation to provide similar mechanical data results for other processes and trends. From the analysis of this study, the following findings can be summarised, as follows.

- From the static analysis of the reeling, it was observed as presented in Fig. 11 that a straight profile was observed then bends a bit which is due to the reeling nature and application of the reeling hose. This is further confirmed by Figs. 12 and 13, where the bending occurs closer to the start of the reeling hose (between 0m and 15m along the arc length of the hose string). This also shows that the results of the static state had some impact on the reeling system, which can be due to the current, winds, vessel motion, added mass, damping, and other factors. This study shows that the material effect of bonded hose properties such as the elastomers used in modelling the hoses can also help to increase its elastic behaviour and durability, thus increasing its capacity, suitability and reeling-ability.
- The global analysis of the reeling hose operation has been carried out to investigate the effect of effective tension, bending moment, curvature and fluid content in the dynamic analysis of the marine bonded hose. The hose behaviour in Figs. 13, 27 and 34 show that the effective tension was maximum at the end that is attached to the reeling vessel. Also, the load response on the reeling hose shows that as it reels, the curvature of the hose also shows that the floatation foam embedded in the hose acts as embedded floats inside the hose, which also impacts upon the stresses on the reeling hose.
- In Fig. 14, the bending moment was reduced to capture up to 200kNm, but the bending moment distribution along the arc length appears to be undulating, due to the connections attached to the hose at the hose ends. The maximum curvature of the hose in Fig. 15 was below 1 rad/m which shows it is fit for use, according to OCIMF GMPHOM [40]. From the selected profiles, the maximum effective tension obtained was 894 kN, as in Fig. 16. It can be concluded that the ends of the hoses need to be highly reinforced as the tensions between 0 and 15m are high. However, it is necessary to investigate the stresses along those sections.
- From Tables 13 and it can be seen that the hose profiles observed were maximum under the reinforced hose type in 0° wave heading with a tension of 1,557 kN and an allowable tension of 4199 kN under the seawater condition, while the least was the mainline hose type in 90° wave heading with a tension of 952 kN and an allowable tension of 3418 kN under the freshwater condition. Thus, it shows that the hose is fit for use as designed and that the strength of the hose is of good capacity. The assessment conducted on the hose strength from the critical load combination showed satisfactory performance. However, more studies on the local design based on burst and collapse loads, liner wrinkling, micro-cracking and metal-composite interface (MCI) are recommended in further research.
- In the parametric analysis with simulation timesteps in Fig. 28, the maximum effective tension has good agreement for the time steps 0.1s, 0.001s and 0.0001s, which also validates the model, especially as the simulations are usually unstable under very high stress values at the top end of the hoses, plus, since the time at 0.1s was faster, and also more stable, as was used for the model. With the stable result obtained from the effective tension profile, thus, it was an additional approach used to validate the model which showed good agreement on the model. This study also showed that the Orcaflex software [65,67] used in this study is validated, as the results were also consistent, as presented.
- From Fig. 17, the maximum bending strain is about 15 % due to the weight of the reeling hose string, the connection ends, the connectors, the MBCs at the hose mid-sections and HEV at the hose end. While the strain value is marginally high, it reasonable to have further FEA to ascertain the impact of that high bending strain. However, it is likely due to the weight of the components of the hose-line, considering the direction is vertically downwards, as seen in Fig. 1(a).
- From Fig. 18, it can be seen that the direct tensile strain has both positive value and negative value. It shows that the hose direct tensile strain could be compressive strain from arc length of 200m–350m. The negative direct tensile strain reflects the presence of

compressive strain. However, this requires further works using experiments or FEA to confirm that the hose will experience pure compression in those sections, and that will enable operators to understand the implication of that negative value for buckling.

- In Fig. 19, the pipelay von Mises strain had the widest margin of variance. This could also indicate the behaviour of the material, or material properties used for the calculation considered in the von Mises strain, but it shows profiles of the strained and unstrained regions. Due to the locus of the yield stress on the hose section being reeled, the hose material had a plastic behaviour that was observed after reeling. As such, these three methods of assessing strains are considered to show good agreement. It is noteworthy to state that the reel-laying subjects the pipeline to large bending which induces plastic strain reversals as the pipeline is reeled on and off followed by aligning and straightening before exiting the installation vessel as also seen in this study. However, there are various aspects to reeling operations that result in various phenomena like wrinkling, pipeline strains, ovality, Lüders band clusters periodicity, external sheath cracks, and other issues due to winding/unwinding, etc. ([20,21,26,53,71–73]).
- Also, regarding the von Mises strain in Fig. 19, it can be observed that it is more than 25 % at the other end of the hose-string, which is where the HEV is connected. This is likely due to the weight of the HEV which is 6.9te, alongside its swivel, and can be high for the hose materials in that section of the reeling hose-string called the reinforced hose end. However, further work is recommended to ascertain the von Mises strain during pipelaying to see the strain distribution across the hose-string by considering the allowable strain for the marine hose.
- Another aspect is the impact of the stress distribution on the reeling hose-string. The maximum von Mises stress shown in Fig. 22 is only 10 MPa, which is noticed at the connection point of the hose, where it meets the reeling drum. This is also noticed in Fig. 34, which reflects the region of the hose that experiences high tension and bending too. To further confirm how applicable and reasonable the stress value of the reeling hose can be utilised, further FEA is recommended by also considering the tensile strength of the hose.
- Lastly, it is noteworthy to state that the maximum tension, maximum bending moment and maximum curvature values presented in Table 13, as well as in Tables 15–18, were obtained from the middle part of the hose. It is evident that both the reinforced part and end fitting part of the hose string have a higher bending moment and curvature thus it is recommended that it should be reinforced better.

5. Conclusion

This study presents a numerical investigation of the marine bonded hoses under three different operations. The load response and parametric studies of marine bonded hoses have been presented under free-standing and reeling operations. It aims to understand the load response, tension profiles, stress profiles, strain distribution and hose curvature of marine reeling hoses. This study also investigates the global design, material modelling, reeling modelling, and parametric relationships for the load response of the bonded hoses. This study suggests new designs that will aid hose designers. Also, the numerically viewed results are helpful for hose manufacturers, and field users of similar reeling models. The developed parametric profiles can also be used to aid safe operation envelopes.

The developed model highlights include the following: firstly, a model on the global design of marine reeling hoses under different environmental conditions with detailed stress profiles. The second novelty is the determination of parameters for validating numerical marine reeling hose systems. Thirdly, the load response of marine bonded hoses with profiles of tensions, bending moment, curvature, strains, bending stress and von Mises stress. Thus, profiles obtained from the Finite Element Analysis (FEA) were presented, as another strain estimation method like the Accumulated Plastic Strain (EPS). However, the response study on the effect of other parameters like contact pressure from fluid content on the marine hose which comes from either the load of the tensioner, or other reeled sections of the hose while on the reel drum, or the vessel load response can be further investigated. Fourthly is the application of a novel cylindrical FPSO on reeling hoses in marine environments.

In this study, a global design was presented on a novel reeling hose. While this has more industry application, findings have been expatriated to detail material behaviour and unique characteristics of the reeling hose. However, the study does not determine a general reeling hose model, due to differences in environmental loads, vessel positions, hose length, hose dimensions and modelling tools. This includes a novelty in the finite element material modelling of marine bonded hose used in the global design. Lastly, the reeling modelling was presented using a detailed study of marine hose lines using Orcaflex, including the effect of fluid on the hose utilization and its implications on the reeling hose. The study has high relevance in the dynamic behaviour of reeling hose studies.

Funding

The School of Engineering, Lancaster University, UK and EPSRC Doctoral Training Centre (DTC), UK are highly appreciated. In addition, the funding of Overseas Scholarships by Niger Delta Development Commission (NDDC), Nigeria as well as the funding support of UNITEN's BOLD25 Initiative, Malaysia are also acknowledged and appreciated.

CRediT authorship contribution statement

Chiemela Victor Amaechi: Conceptualization, Data curation, Formal analysis, Funding acquisition, Investigation, Methodology, Project administration, Resources, Software, Supervision, Validation, Visualization, Writing – original draft, Writing – review & editing. **Ahmed Reda:** Formal analysis, Funding acquisition, Investigation, Methodology, Project administration, Resources, Software, Supervision, Validation, Visualization, Writing – review & editing. **Mohamed A. Shahin:** Formal analysis, Funding acquisition, Investigation, Methodology, Project administration, Resources, Software, Supervision, Validation, Visualization, Writing – review &

editing. **Charles Agbomerie Odijie:** Conceptualization, Data curation, Formal analysis, Funding acquisition, Investigation, Methodology, Project administration, Resources, Software, Supervision, Validation, Visualization, Writing – original draft, Writing – review & editing. **Salmia Binti Beddu:** Formal analysis, Funding acquisition, Investigation, Methodology, Project administration, Resources, Software, Supervision, Validation, Visualization, Writing – review & editing. **Daud bin Mohamad:** Formal analysis, Funding acquisition, Investigation, Methodology, Project administration, Resources, Software, Supervision, Validation, Visualization, Writing – review & editing. **Agusril Syamsir:** Formal analysis, Funding acquisition, Investigation, Methodology, Project administration, Resources, Software, Supervision, Validation, Visualization, Writing – review & editing. **Idris Ahmed Ja'e:** Formal analysis, Funding acquisition, Investigation, Methodology, Project administration, Resources, Software, Supervision, Validation, Visualization, Writing – review & editing. **Xuanze Ju:** Formal analysis, Funding acquisition, Investigation, Methodology, Project administration, Resources, Software, Supervision, Validation, Visualization, Writing – review & editing.

Declaration of competing interest

The authors declare no conflict of interest in this research. The funders had no hand in the determination of the results.

Data availability

The data that has been used is confidential.

Acknowledgements

The authors acknowledge the technical and the institutional supports with computational resources. The technical support from industry experts was much helpful. The permission obtained from Orcina to use/adapt the Orcaflex line theory in Fig. 5 is well appreciated. The feedback from the journal editor and the reviewers is well appreciated as it has helped to improve the quality of this manuscript.

References

[1] Amaechi CV, Wang F, Ja'e IA, Aboshio A, Odijie AC, Ye J. A literature review on the technologies of bonded hoses for marine applications. Ships Offshore Struct 2022;17(12):2819–50. https://doi.org/10.1080/17445302.2022.2027682.
[2] Amaechi CV, Reda A, Shahin MA, Sultan IA, Beddu SB, Ja'e IA. State-of-the-art review of composite marine risers for floating and fixed platforms in deep seas. Appl Ocean Res 2023;138:103624. https://doi.org/10.1016/j.apor.2023.103624.
[3] Mao Y, Yang Z, Wang G, Chen J, Yan J, Wang Z. A study on the mechanical behavior of umbilical cables under impact loads using experimental and numerical methods. *Marine Structures* 2025;*99*:103700. https://doi.org/10.1016/j.marstruc.2024.103700.
[4] Reda A, Howard IM, Forbes GL, Sultan IA, McKee. K.Design and installation of subsea cable, pipeline and umbilical crossing interfaces. *Engineering Failure Analysis* 2017;*81*:193–203. https://doi.org/10.1016/j.engfailanal.2017.07.001.
[5] Ochoa O, Salama M. Offshore composites: transition barriers to enabling technology. Compos Sci Technol 2005;65(15–16):2588–96. https://doi.org/10.1016/j.compscitech.2005.05.019.
[6] Saparuddin S, Assidiq FM. Analysis of motion and mooring of FPSO vessels due to different types of mooring material. Maritime Park Journal of Maritime Technology and Society 2024;3(1):12–20. https://doi.org/10.62012/mp.v3i1.31721.
[7] OCIMF. Single point mooring maintenance and operations guide (SMOG). Oil Companies international marine Forum (OCIMF). London, UK: Witherby & Co. Ltd; 1995.
[8] OCIMF. A study into crane loads associated with hose handling at offshore terminals, *OCIMF info paper*, October Issue, version 6. London, UK: Oil Companies International Marine Forum (OCIMF); 2020. p. 1–35. https://www.ocimf.org/document-libary/108-a-study-into-crane-loads-associated-with-hose-handling-at-offshore-terminals/file.
[9] Amaechi CV, Wang F, Hou X, Ye J. Strength of submarine hoses in Chinese-lantern configuration from hydrodynamic loads on CALM buoy. Ocean Eng 2019;171 (2019):429–42. https://doi.org/10.1016/j.oceaneng.2018.11.010. 2019.
[10] Wei D, An C, Zhang J, Huang Y, Gu C. Effect of winding steel wire on the collapse pressure of submarine hose. J Mar Sci Eng 2022;10(10):1365. https://doi.org/10.3390/jmse10101365.
[11] Gao S, An C, Wei D, Estefen SF, Li Y. Bursting failure modes of double carcass floating hose. Ocean Eng 2024;294:116822. https://doi.org/10.1016/j.oceaneng.2024.116822.
[12] Huang G, Wu W. Armored steel wire stress monitoring strategy of a flexible hose in LNG tandem offloading operation. Ocean Eng 2023;281:114775. https://doi.org/10.1016/j.oceaneng.2023.114775.
[13] Gao Q, Zhang P, Duan M, Yang X, Shi W, An C, Li Z. Investigation on the structural behaviour of ring-stiffened composite offshore T-rubber hose under internal pressure. Appl Ocean Res 2018;79(1):7–19. https://doi.org/10.1016/j.apor.2018.07.007.
[14] Toguyeni GA, Banse J. Mechanically lined pipe: installation by reel-lay. In: Paper OTC 23096. Proceedings of the offshore technology conference, Houston, Texas, USA; 2012. https://doi.org/10.4043/23096-MS. 30 April-3 May 2012.
[15] Szczotka M. Pipe laying simulation with an active reel drive. Ocean Eng 2010;37:539–48. https://doi.org/10.1016/j.oceaneng.2010.02.009.
[16] Szczotka M. Dynamic analysis of offshore pipe laying operation using the reel method. Acta Mech Sin 2011;27(1):44–55. https://doi.org/10.1007/s10409-011-0400-9.
[17] Zhao T, Hu Z. Numerical analysis of detaching and wrinkling of mechanically lined pipe during its spooling-on stage to the reel. Theoretical and Applied Mechanics Letters 2015;5:205–9. https://doi.org/10.1016/j.taml.2015.08.004. 2015.
[18] Yuxin X, Pan F, Yong B. Mechanical behaviour of metallic strip flexible pipes during reeling operation. Mar Struct 2021;77:102942. https://doi.org/10.1016/j.marstruc.2021.102942. 2021.
[19] Palmer AC, King RA. Subsea pipeline engineering. second ed. USA: PennWell Corporation; 2008.
[20] Guo B, Song S, Chacko J, et al. Offshore pipelines. UK: Elsevier Publishers; 2005.
[21] Dawood AA. A study of pipeline response during reel-lay installation. In: Masters thesis, faculty of engineering and applied science. St John's Newfoundland, Canada: The Memorial University of Newfoundland; 2014. Memorial University of Newfoundland, https://research.library.mun.ca/8055/1/thesis.pdf.
[22] PSA & 4Subsea. Bonded Flexibles – state-of-the-art bonded flexible pipes 0389-26583-U-0032, Revision 5, For PSA Norway. 2018. https://www.4subsea.com/wp-content/uploads/2019/01/PSA-Norway-State-of-the-art-Bonded-Flexible-Pipes-2018_4Subsea.pdf.

[23] Amaechi CV, Chesterton C, Butler HO, Wang F, Ye J. Review on the design and mechanics of bonded marine hoses for Catenary Anchor Leg Mooring (CALM) buoys. Ocean Eng 2021;242:110062. https://doi.org/10.1016/j.oceaneng.2021.110062.

[24] Wang C, Sun M, Shankar K, Xing S, Zhang L. CFD simulation of vortex-induced vibration for FRP composite riser with different modeling methods. Appl Sci 2018;8589. https://doi.org/10.3390/app8050684.

[25] PSA & 4Subsea. Un-bonded flexible risers – recent field experience and actions for increased robustness. 0389-26583-U-0032, Revision 5, For PSA Norway. https://www.ptil.no/contentassets/c2a5bd00e8214411ad5c4966009d6ade/un-bonded-flexible-risers–recent-field-experience-and-actions–for-increased-robustness.pdf, 2013.

[26] Bai Y, Bai Q. Subsea pipeline and risers. UK: Elsevier Publishers; 2005. https://doi.org/10.1016/B978-0-08-044566-3.X5000-3.

[27] Chesterton C. A global and local analysis of offshore composite material reeling pipeline hose, with FPSO, mounted reel drum. BEng Dissertation. UK: Lancaster University, Engineering Department; 2020.

[28] Gao P, Li C, Wang H, Gao Q, Li Y. A simplified method to predict the crush behavior of offshore bonded rubber hose. J Mar Sci Eng 2023;11:406. https://doi.org/10.3390/jmse11020406. 2023.

[29] Fergestad D, Løtveit SA. Handbook on design and operation of flexible pipes. Sintef MARINTEK/NTNU/4Subsea; 2014. 978-82-7174-265-2, https://core.ac.uk/download/pdf/52134083.pdf.

[30] Focke ES. Reeling of tight fit pipe. PhD Thesis. Delft University of Technology; 2007. Offshore Engineering, report 2007.OE.010, http://resolver.tudelft.nl/uuid:21348ba3-bce9-4b01-98fd-f1a32fafaaa9.

[31] Manouchehri S. A discussion of practical aspects of reeled flowline installation. In: Proceedings of the ASME 2012 31st international conference on ocean, offshore and arctic engineering OMAE2012 june 10-15, 2012, Rio de Janeiro, Brazil; 2012. Paper OMAE2012-83649, http://cyrusogr.com/files/OMAE2012-83649.pdf.

[32] Lassen T, Lem AI, Imingen G. Load response and finite element modelling of bonded offshore loading hoses. In: Proceedings of the ASME 2014 33rd international conference on ocean. San Francisco, California, USA: Offshore and Arctic Engineering; 2014. https://doi.org/10.1115/OMAE2014-23545. OMAE2014, June 8-13, 2014.

[33] Ju X, Amaechi CV, Dong B, Meng X, Li J. Numerical analysis of fishtailing motion, buoy kissing and pullback force in a catenary anchor leg mooring (CALM) moored tanker system. Ocean Eng 2023;278:114236. https://doi.org/10.1016/j.oceaneng.2023.114236.

[34] HSE UK and NobleDenton. Floating production system: JIP FPS mooring integrity. Prepared by noble denton europe limited for the health and safety executive 2006. Health and Safety Executieve (HSE) UK's Research Report 444, https://www.hse.gov.uk/research/rrpdf/rr444.pdf; 2006.

[35] Jean P, Goessens K, L'Hostis D. Failure of chains by bending on deepwater mooring systems. Proceedings of offshore technology conference. 2005. https://doi.org/10.4043/17238-MS. Houston, Texas, May 2005.

[36] Safety4Sea. Unsafe operations at offshore tanker loading berth. Published on August 20, 2012, in the Accidents Section, https://safety4sea.com/unsafe-operations-at-offshore-tanker-loading-berth/; 2012.

[37] Edward C, Dev DA. Assessment of CALM buoys motion response and dominant OPB/IPB inducing parameters on fatigue failure of offshore mooring chains. In: Okada T, Suzuki K, Kawamura Y, editors. Practical design of ships and other floating structures. PRADS 2019. Lecture notes in civil engineering, vol. 64. Singapore: Springer; 2021. https://doi.org/10.1007/978-981-15-4672-3_35.

[38] Asmara IPS, Sumardiono, Wibowo VAP. Safety analysis of mooring hawser of FSO and SPM buoy in irregular waves. In: Maritime safety international conference, IOP conf. Series: earth and environmental science, vol. 557. IOP Publishing; 2020. p. 1–9. https://doi.org/10.1088/1755-1315/557/1/012003 (2020) 012003.

[39] API. API 17K; Specification for bonded flexible pipe. third ed. Texas, USA: American Petroleum Institute; 2017 (API).

[40] OCIMF. Guide to manufacturing and purchasing hoses for offshore moorings (GMPHOM). Oil Companies international marine Forum (OCIMF). Livingstone, UK: Witherby Seamanship International Ltd.; 2009.

[41] Santos AMP, Soares CG. Cost optimization of shuttle tanker offloading operations. Ocean Eng 2024;301:117378. https://doi.org/10.1016/j.oceaneng.2024.117378.

[42] Araújo JB, Fernandes AC, Jr JSS, Thurler AC, Vilela AM. Innovative oil offloading system for deep water. In: Proceedings of the offshore technology conference; 2019, D022S057R006. https://doi.org/10.4043/29443-MS. Houston, Texas, May 2019.

[43] Breivik KG. Experience with offloading in the North Sea, Development of new cost efficient technology for marine storage and production. In: Proceedings of the offshore technology conference; 1995, May. https://doi.org/10.4043/7723-MS. OTC-7723).

[44] Tannuri EA, Kubota LK, Pesce CP. Adaptive control strategy for the dynamic positioning of a shuttle tanker during offloading operations. J. Offshore Mech. Arct. Eng 2006;128(3):203–10. https://doi.org/10.1115/1.2199559. August 2006.

[45] Rodriguez CEP, de Souza GFM, Gilberto FM, Martins MR. Risk-based analysis of offloading operations with FPSO production units. In: Proceedings of the 20th international congress of mechanical engineering. Brazil: Gramado; 2009, January. https://www.researchgate.net/profile/Marcelo-Ramos-Martins/publication/290607678.

[46] Dareing DW. Mechanics of drillstrings and marine risers. New York, USA: ASME Press; 2012. https://doi.org/10.1115/1.859995.

[47] Wang F, Chen J, Gao S, Tang K, Meng X. Development and sea trial of real-time offshore pipeline installation monitoring system. Ocean Eng 2017;146:468–76. https://doi.org/10.1016/j.oceaneng.2017.09.016. 1 December 2017.

[48] Amaechi CV. Novel design, hydrodynamics and mechanics of marine hoses in oil/gas applications. Engineering department. UK: Lancaster University; 2022. PhD Thesis.

[49] MatWeb. MatWeb- material property data [Online], https://www.matweb.com/search/PropertySearch.aspx; 2024.

[50] ISO. ISO 13628-10:2005 Petroleum and natural gas industries-Design and operation of subsea production systems-Part 10: specification for the bonded flexible pipe. Geneva, Switzerland: International Organization for Standardization; 2005.

[51] O'Donoghue T. The dynamic behaviour of a surface hose attached to a CALM buoy. Edinburgh, U.K: Heriot-Watt University; 1987. PhD Thesis, https://www.ros.hw.ac.uk/handle/10399/1045.

[52] DNV. Offshore standard: DNV-ST-F101 submarine pipeline systems. Oslo, Norway: Det Norske Veritas; 2021.

[53] Kyriakides S, Corona E. Mechanics of offshore pipelines, vol. 1. UK: Elsevier Publishers; 2007. *Buckling and Collapse*.

[54] API. API RP 2SK; Design and analysis of stationkeeping systems for floating structures. third ed. Texas, USA: American Petroleum Institute; 2005 (API).

[55] Chen Y, Tan LB, Jaiman RK, Sun X, Tay T, Tan VBC. Global-local analysis of a full-scale composite riser during vortex-induced vibration. In: Proceedings of the ASME 2013 32nd international conference on ocean, offshore and arctic engineering, vol. 7; 2013. https://doi.org/10.1115/OMAE2013-11632. *CFD and VIV*. Nantes, France. June 9–14, 2013. V007T08A084.

[56] DNV. *Offshore standard: dynamic risers DNV-OS-F201*, october. Oslo, Norway: Det Norske Veritas; 2010.

[57] Lipski W. Mechanically lined pipe - installation by reel-lay 2011:17. https://www.yumpu.com/en/document/read/26877695/mechanical-lined-pipe-installation-by-reel-lay-subsea-uk.

[58] Taams V.J. *The onset of pipeline twist during reel-lay operations.* Delft University of Technology, Offshore and Dredging Engineering, 2016. MSc Thesis. http://resolver.tudelft.nl/uuid:9edd02a2-956f-414d-83c8-dae8b928f585.

[59] Muspratt A. Guide to FPSO (Floating Production Storage and Offloading), https://www.oilandgasiq.com/fpso-flng/articles/guide-to-floating-production-storage-and-offloading-FPSO; 2018.

[60] O'Donoghue T, Halliwell AR. Vertical bending moments and axial forces in a floating marine hose-string. Eng Struct 1990;12(4):124–33. https://doi.org/10.1016/0141-0296(90)90018-N.

[61] Castello, X., Estefen, S. F. Limit strength and reeling effects of sandwich pipes with bonded layers. *International journal of mechanical sciences*, 2007; *49*(5), 577-588. https://doi.org/10.1016/j.ijmecsci.2006.09.015.

[62] Odijie AC, Ye J. Effect of vortex-induced vibration on a paired-column SemiSubmersible platform. Int J Struct Stabil Dynam 2015;15(8). https://doi.org/10.1142/S0219455415400192.

[63] Odijie AC, Quayle S, Ye J. Wave-induced stress profile on a paired column semisubmersible hull formation for column reinforcement. Eng Struct 2017;143 (April):77–90. https://doi.org/10.1016/j.engstruct.2017.04.013.
[64] O'Donoghue T, Halliwell AR. Floating hose-strings attached to A calm buoy. In: Proceedings of the offshore technology conference, Houston, Texas; 1988. https://doi.org/10.4043/5717-MS. May 1988. Paper Number: OTC-5717-MS.
[65] Orcina. *OrcaFlex manual, version 11.0f*, ulverston. Cumbria, UK: Orcina Ltd; 2014.
[66] McCann S, Evans D, Bannister A, Tan H. Effects of reeling on the mechanical properties of HFI welded pipes. In: 4th pipeline technology conference 2009; 2009, 200309. .pipeline-conference.com/sites/default/files/papers/PTC%202009%201.2%20Mc%20Cann.pdf.
[67] Orcina. Orcaflex documentation. Version 11.0f. [Online], https://www.orcina.com/webhelp/OrcaFlex/Default.htm; 2021.
[68] DNVGL. DNVGL-OS-E403 offshore loading buoys. Oslo, Norway: Det Norske Veritas & Germanischer Lloyd; 2015. no. July.
[69] DNVGL. DNVGL-RP-F205 Global performance analysis of deepwater floating structures. Oslo, Norway: Det Norske Veritas & Germanischer Lloyd; 2017. no. June.
[70] DNVGL. DNVGL-RP-N103 Modelling and analysis of marine operations. Oslo, Norway: Det Norske Veritas & Germanischer Lloyd; 2017. no. July.
[71] Xu W, Li Z, Yuan L, Xu A. On the effect of stiffness discontinuities on the reeling of pipelines using FEM and machine learning strategy. *Ships and Offshore Structures* 2024:1–10. ahead-of print version, https://doi.org/10.1080/17445302.2024.2355402.
[72] Zhang W, Kyriakides S. Winding and unwinding a pipe with lüders bands on a reel part I: Analysis of base case. *International Journal of Solids and Structures* 2024; *290*:112687. https://doi.org/10.1016/j.ijsolstr.2024.112687.
[73] Zhang W, Kyriakides S. Winding and unwinding a pipe with Lüders bands on a reel. Part II: Effect of problem parameters. *International Journal of Solids and Structures* 2024;*291*:112688. https://doi.org/10.1016/j.ijsolstr.2024.112688.